Using computer simulations as “numerical experiments” to understand statistical mechanics

Simulate the configurations of molecules

Stochastic simulation technique ("Monte Carlo") to derive the equation of state for a 2D liquid

THE JOURNAL OF CHEMICAL PHYSICS VOLUME 21, NUMBER 6 JUNE, 1953

Equation of State Calculations by Fast Computing Machines

NICHOLAS METROPOLIS, ARIANNA W. ROSENBLUTH, MARSHALL N. ROSENBLUTH, AND AUGUSTA H. TELLER,
Los Alamos Scientific Laboratory, Los Alamos, New Mexico

AND

EDWARD TELLER,* *Department of Physics, University of Chicago, Chicago, Illinois*

(Received March 6, 1953)

A general method, suitable for fast computing machines, for investigating such properties as equations of state for substances consisting of interacting individual molecules is described. The method consists of a modified Monte Carlo integration over configuration space. Results for the two-dimensional rigid-sphere system have been obtained on the Los Alamos MANIAC and are presented here. These results are compared to the free volume equation of state and to a four-term virial coefficient expansion.

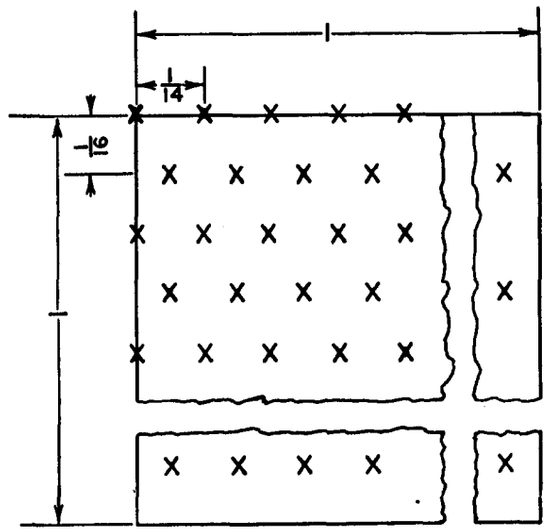

FIG. 2. Initial trigonal lattice.

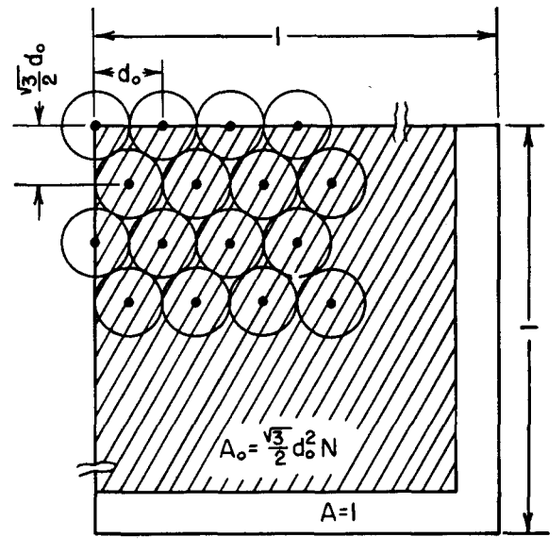

FIG. 3. The close-packed arrangement for determining A_0.

The system

$$E = \frac{1}{2} \sum_{\substack{i=1 \\ i \neq j}}^{N} \sum_{j=1}^{N} V(d_{ij}).$$

(Potential) energy

$$\bar{F} = \left[\int F \exp(-E/kT) d^{2N}p d^{2N}q \right] \Big/ \left[\int \exp(-E/kT) d^{2N}p d^{2N}q \right],$$

Average of some quantity F

Equation of state determined by the numerical MC experiment

$$pV = Nk_BT + \text{corrections}$$ (V = 2D volume)

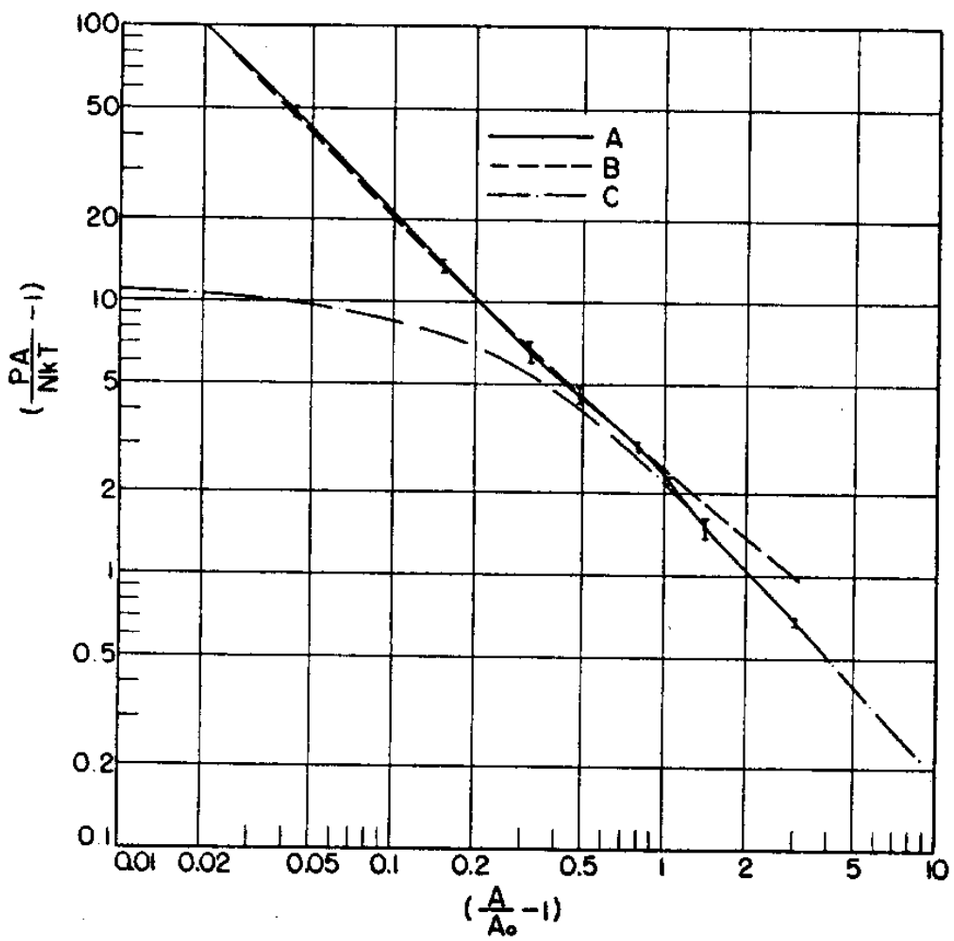

FIG. 4. A plot of $(PA/NkT)-1$ *versus* $(A/A_0)-1$. Curve A (solid line) gives the results of this paper. Curves B and C (dashed and dot-dashed lines) give the results of the free volume theory and of the first four virial coefficients, respectively.

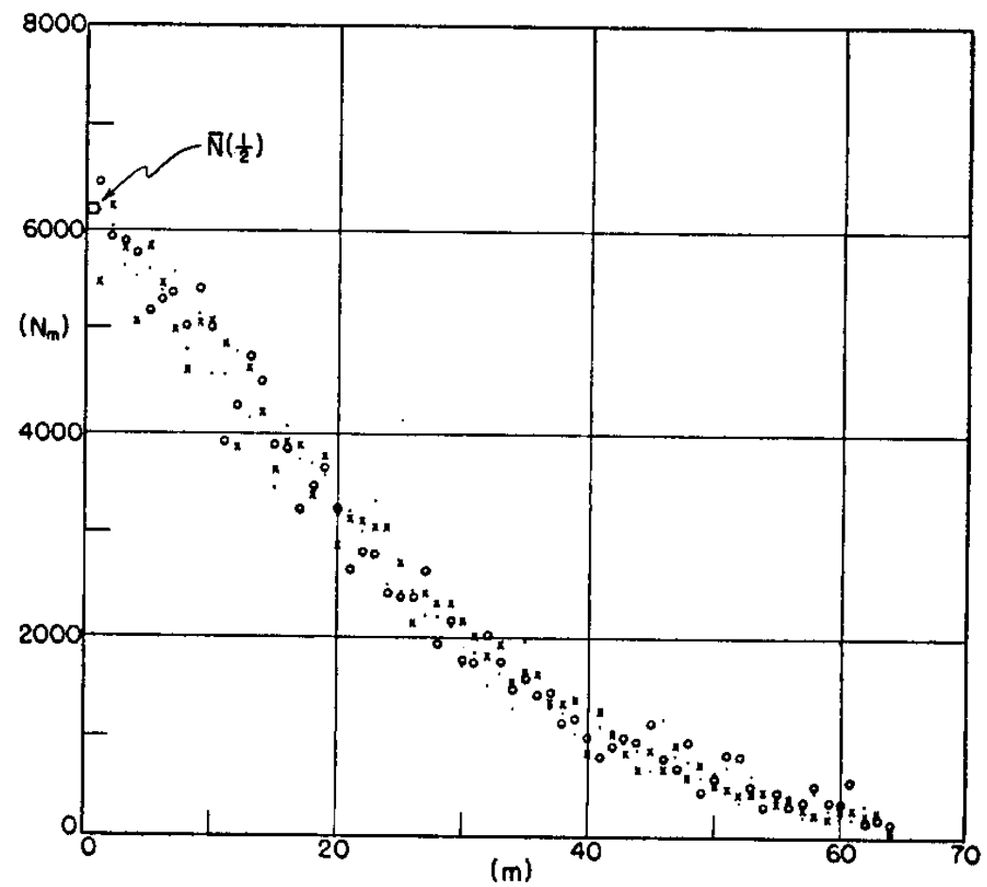

FIG. 5. The radial distribution function N_m for $\nu=5$, $(A/A_0)=1.31966$, $K=1.5$. The average of the extrapolated values of $N_{\frac{1}{2}}$ in $\bar{N}_{\frac{1}{2}}=6301$. The resultant value of $(PA/NkT)-1$ is $64\bar{N}_{\frac{1}{2}}/N^2(K^2-1)$ or 6.43. Values after 16 cycles, ●; after 32, ×; and after 48, ○.

Simulate the dynamics of simple molecules

PHYSICAL REVIEW VOLUME 136, NUMBER 2A 19 OCTOBER 1964

Correlations in the Motion of Atoms in Liquid Argon*

A. RAHMAN
Argonne National Laboratory, Argonne, Illinois
(Received 6 May 1964)

~ 3.6 nm

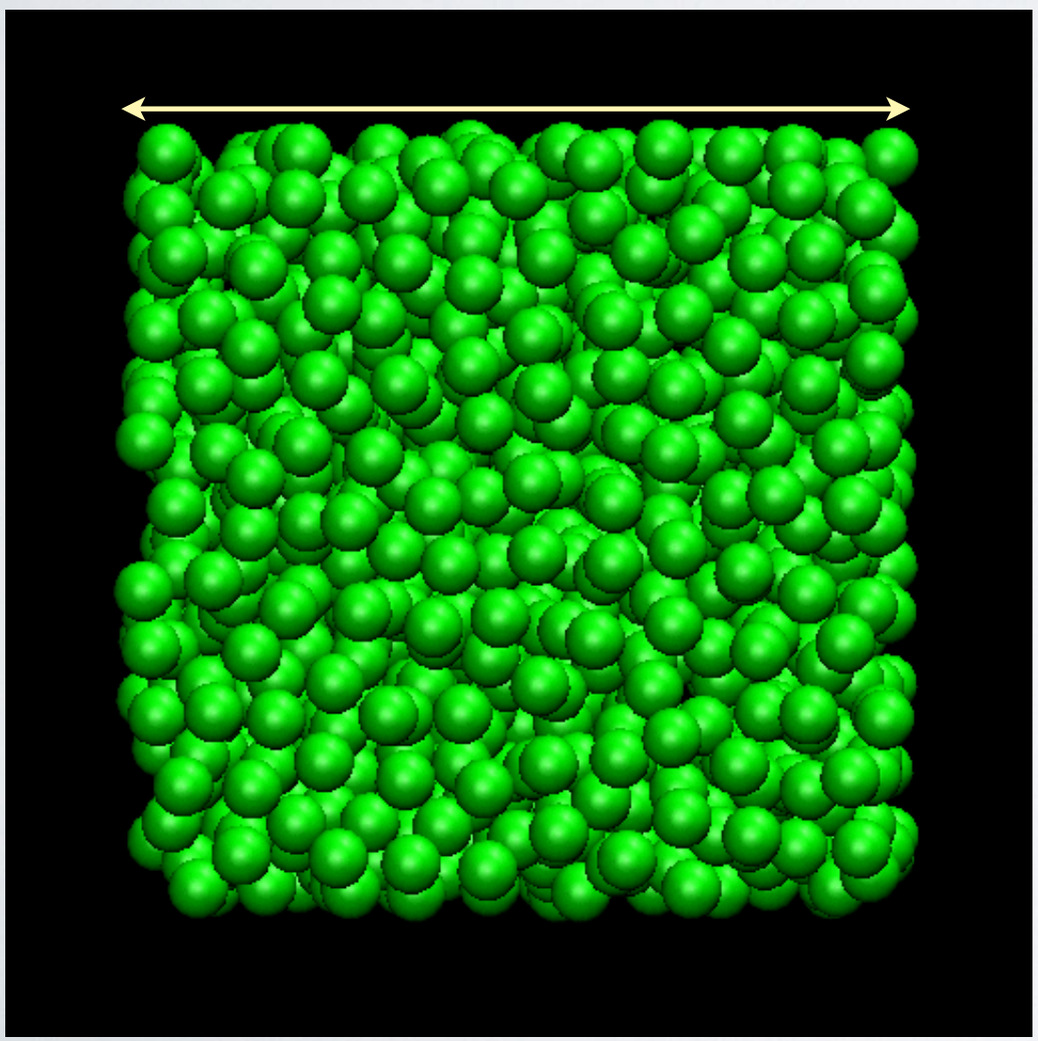

- Solve Newton's equation of motion

$$M_i \ddot{\mathbf{r}}_i = -\frac{\partial U}{\partial \mathbf{r}_i}$$

$$U = \sum_{ij} 4\epsilon \left(\left[\frac{\sigma}{r_{ij}}\right]^{12} - \left[\frac{\sigma}{r_{ij}}\right]^{6} \right)$$

- Discretization and iterative solution itérative yields trajectories = time series (< 100 ns)

$$\mathbf{r}_i(n+1) \leftarrow 2\mathbf{r}_i(n) - \mathbf{r}_i(n-1) + \frac{\Delta t^2}{M_i}\mathbf{F}_i(n)$$

$$\mathbf{v}_i(n) \leftarrow \frac{\mathbf{r}_i(n+1) - \mathbf{r}_i(n-1)}{2\Delta t}.$$

Forces: $\mathbf{F}_i = -\frac{\partial U}{\partial \mathbf{r}_i}$

PHYSICAL REVIEW VOLUME 159, NUMBER 1 5 JULY 1967

Computer "Experiments" on Classical Fluids. I. Thermodynamical Properties of Lennard-Jones Molecules*

LOUP VERLET†
Belfer Graduate School of Science, Yeshiva University, New York, New York
(Received 30 January 1967)

The equation of motion of a system of 864 particles interacting through a Lennard-Jones potential has been integrated for various values of the temperature and density, relative, generally, to a fluid state. The equilibrium properties have been calculated and are shown to agree very well with the corresponding properties of argon. It is concluded that, to a good approximation, the equilibrium state of argon can be described through a two-body potential.

$$V(r)=4\left((\sigma/r)^{12}-(\sigma/r)^{6}\right).$$

interaction potential

$$m\frac{d^2\mathbf{r}_i}{dt^2}=\sum_{j\neq i}\mathbf{f}(r_{ij}).$$

pairwise additive forces

$$\mathbf{r}_i(t+h)=-\mathbf{r}_i(t-h)+2\mathbf{r}_i(t)+\sum_{j\neq i}\mathbf{f}(r_{ij}(t))h^2,$$

Verlet algorithm

Periodic boundary conditions

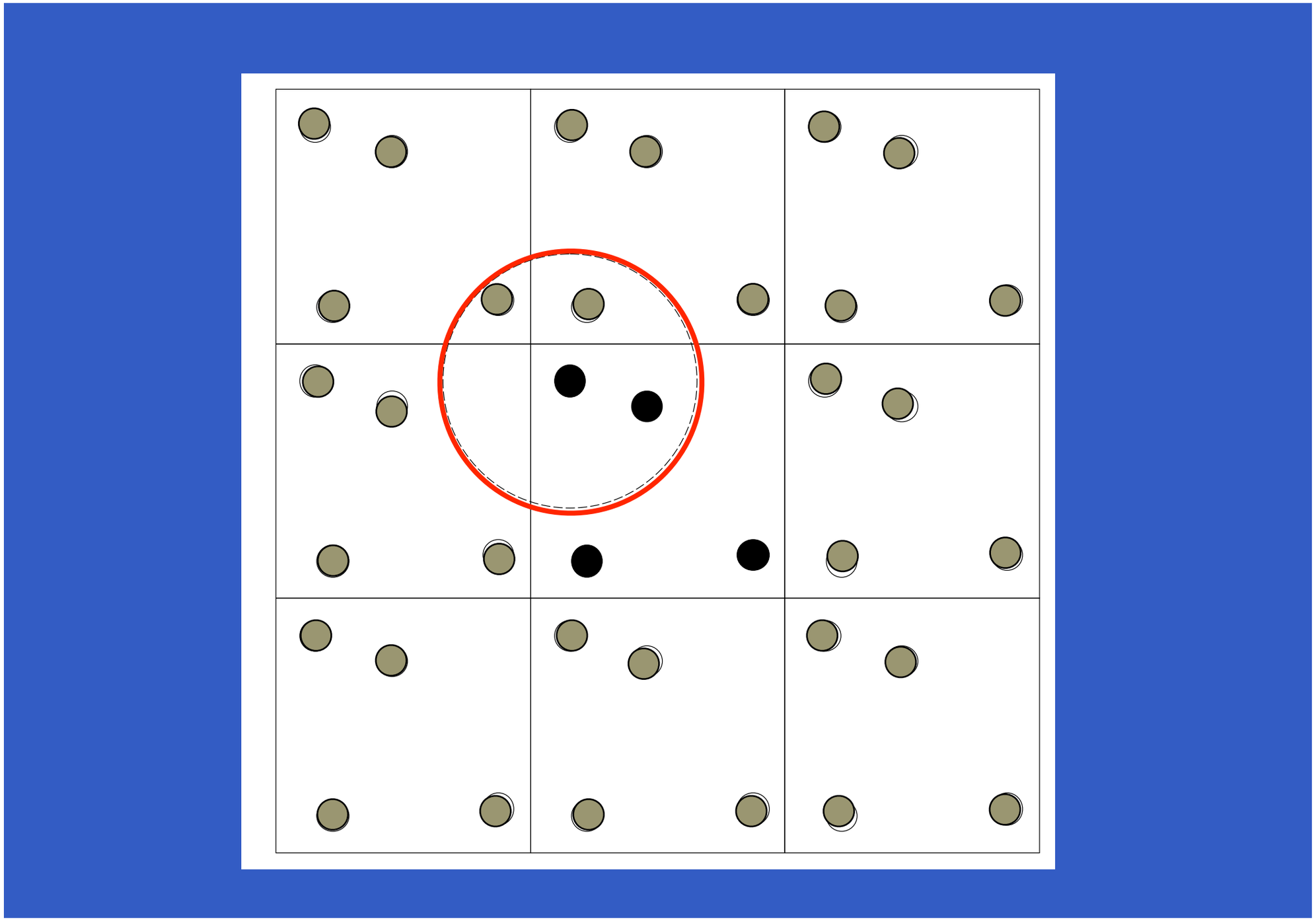

Static pair correlation function

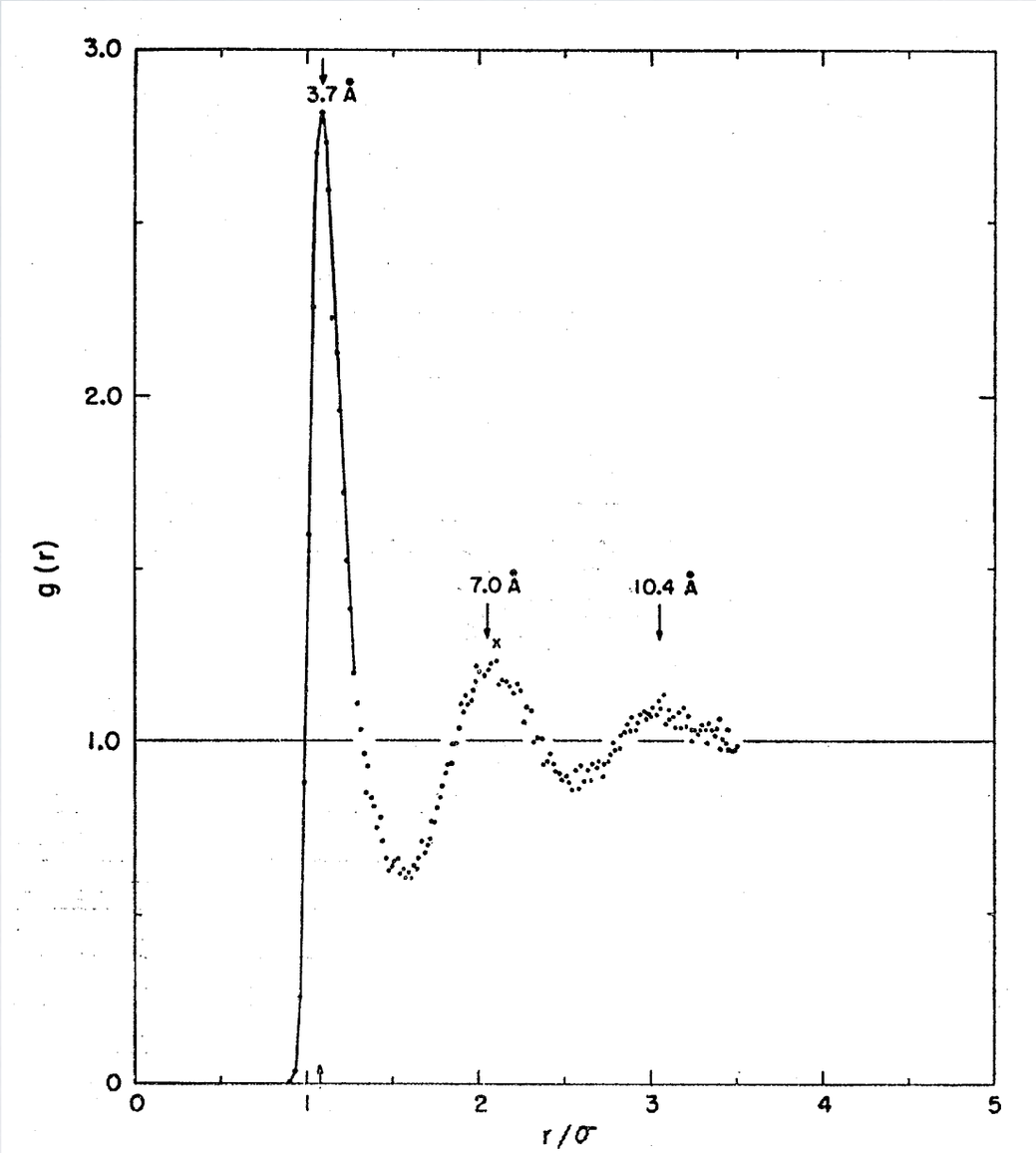

FIG. 2. Pair-correlation function obtained in this calculation at 94.4°K and 1.374 gcm^{-3}. The Fourier transform of this function has peaks at $\kappa\sigma = 6.8$, 12.5, 18.5, 24.8.

$$g(r) = (V/N)[n(r)/4\pi r^2 \Delta r].$$

Measurable by X-ray and neutron diffraction

Maxwell distribution of the velocities and temperature fluctuations

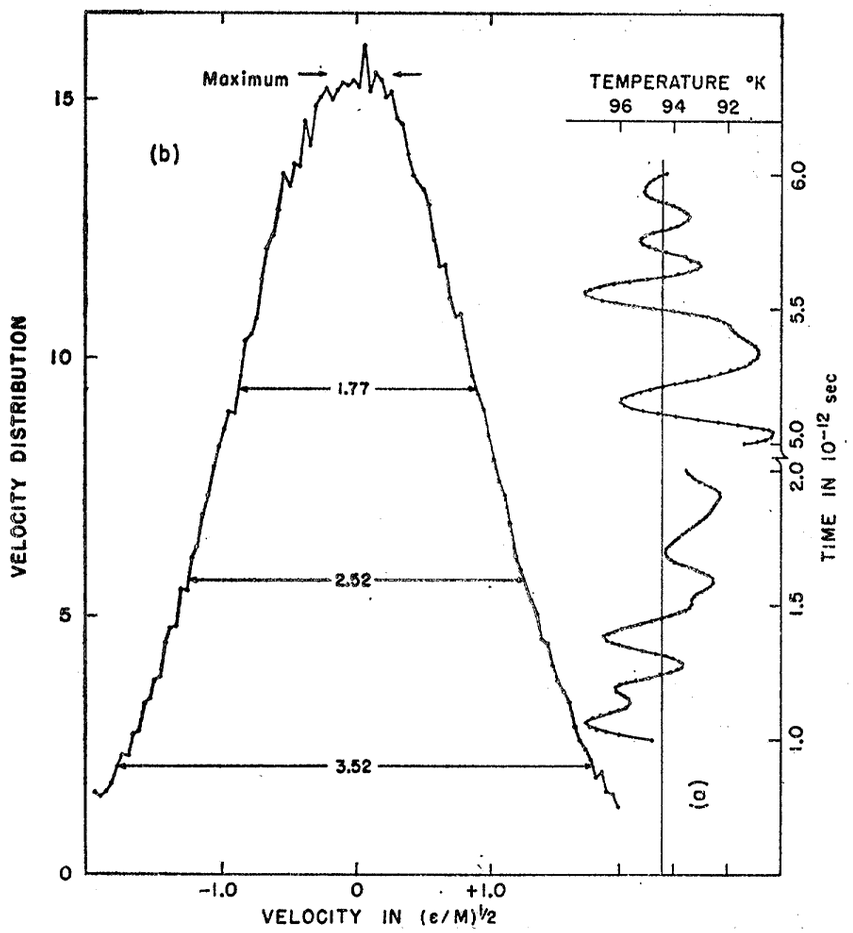

FIG. 1. Fluctuations of temperature with time in two sample regions (curve a); distribution of velocities is shown as curve b; widths of the distribution are shown at $e^{-1/2}$, e^{-1}, and e^{-2} of maximum.

TABLE I. Mean temperature and the rms deviation after ν increments of time have been calculated. The value of the increment $=10^{-14}$ sec.

ν	$\bar{T}$ (°K) for Steps 1 to ν	$(\langle T^2\rangle_{av}-\bar{T}^2)^{1/2}/\bar{T}$
100	94.64	0.0167
200	94.47	0.0161
300	94.55	0.0158
400	94.55	0.0155
500	94.67	0.0160
600	94.51	0.0170
700	94.43	0.0170
780	94.45	0.0165

Time-dependent mean squared displacement

n=2

$$\langle r^{2n}\rangle = \frac{1}{N}\sum_{i=1}^{N}[\mathbf{r}_i(t)-\mathbf{r}_i(0)]^{2n}, \quad n=1, 2, 3, 4.$$

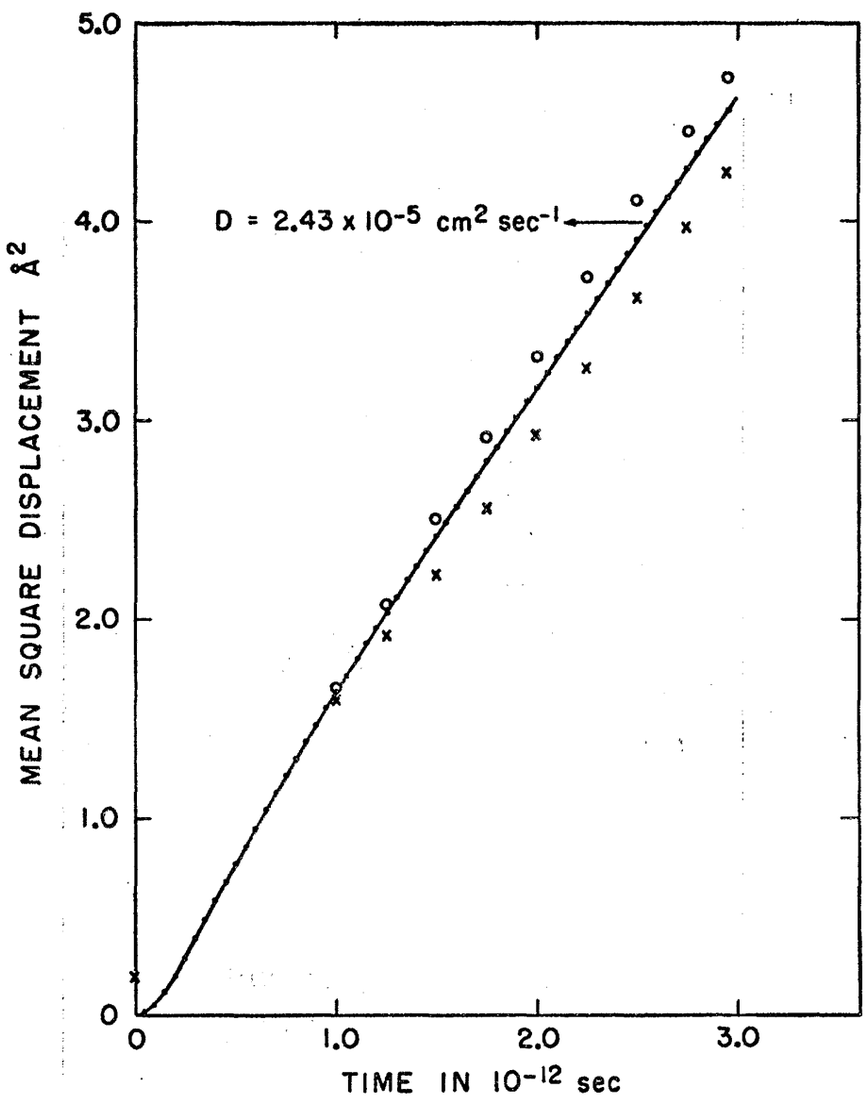

FIG. 3. Mean-square displacement of particles. The continuous curve is the mean of a set of 64 curves; the two members of the set which have *maximum* departures from the mean are shown as circles and as crosses. The asymptotic form of the continuous curve is $6Dt+C$, with D as shown on the figure and $C=0.2$ Å^2.

Measurable by thermal neutron scattering

Velocity autocorrelation function

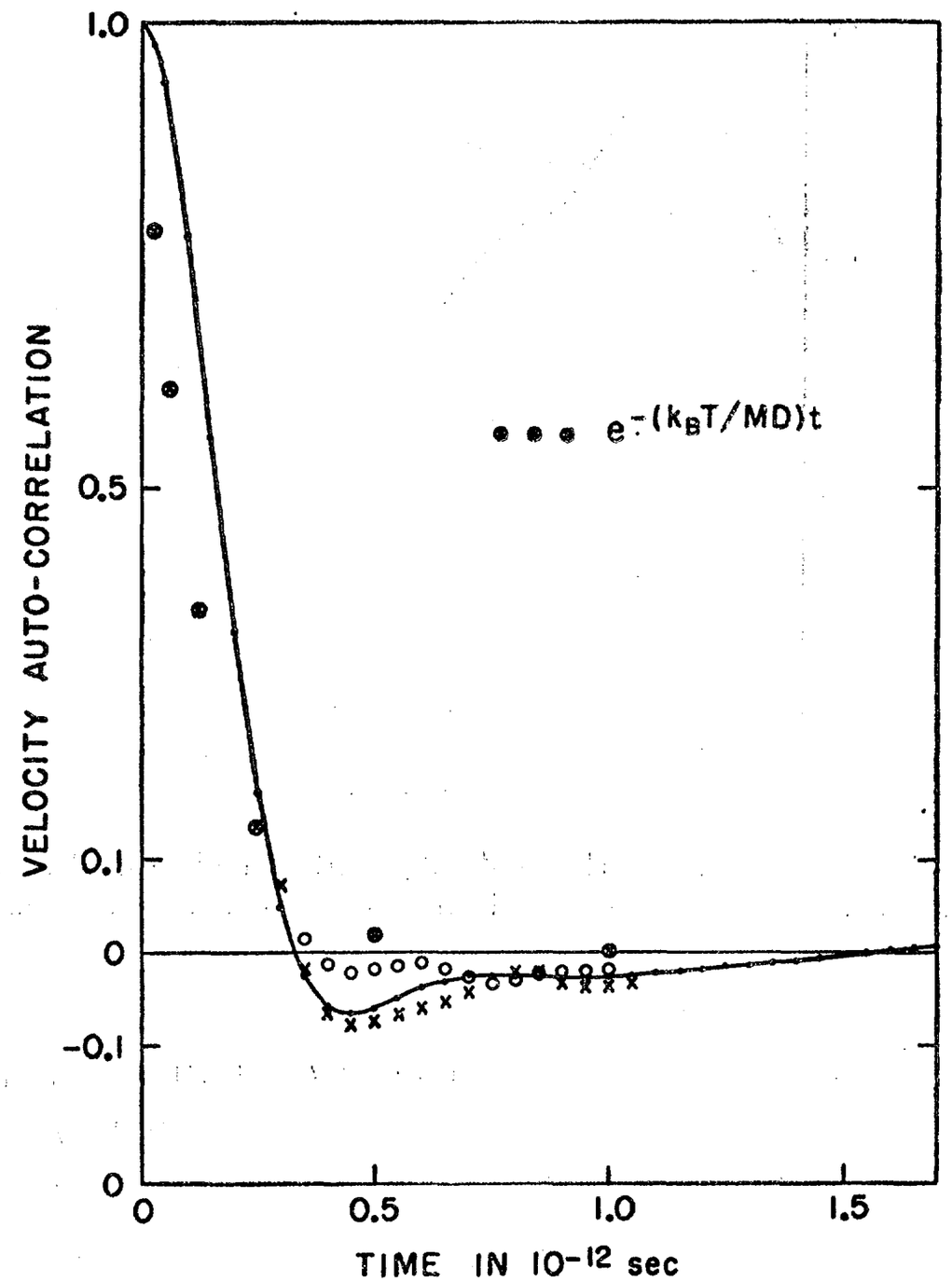

FIG. 4. The velocity autocorrelation function. The Langevin-type exponential function is also shown. The continuous curve, the circles, and the crosses correspond to the curves shown in Fig. 3.

$$\langle \mathbf{v}(0)\cdot\mathbf{v}(t)\rangle = \frac{1}{N}\sum_{i=1}^{N} \mathbf{v}_i(0)\cdot\mathbf{v}_i(t)\,.$$

Measurable by thermal neutron scattering

Velocity autocorrelation function — Fourier transform

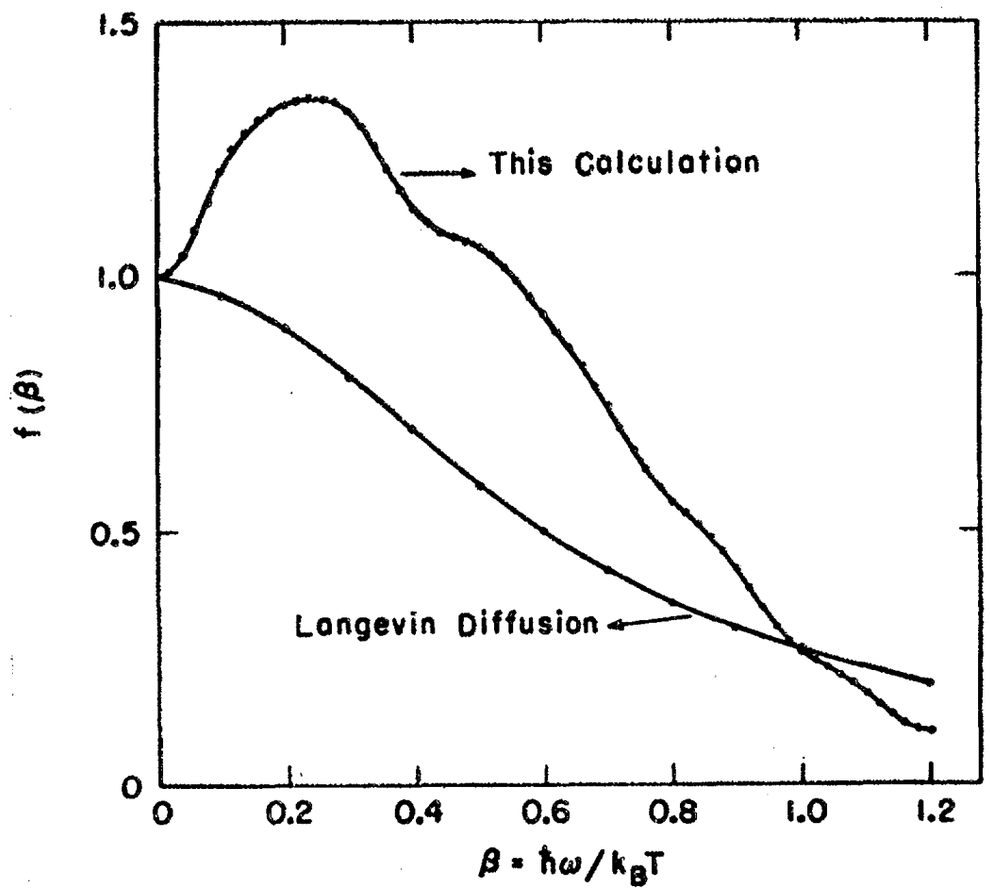

FIG. 5. Spectrum of the velocity autocorrelation function. The Lorentzian spectrum of a Langevin-type correlation is also shown.

$$f(\omega)=\frac{kT}{MD}\int_0^\infty \frac{\langle \mathbf{v}(0)\cdot\mathbf{v}(t)\rangle}{\langle \mathbf{v}^2\rangle}\cos\omega t dt$$

$$f(\beta)=\lambda\int_0^\infty \frac{\langle \mathbf{v}(0)\cdot\mathbf{v}(u)\rangle}{\langle \mathbf{v}^2\rangle}\cos\beta u du\,.$$

Dynamics of water

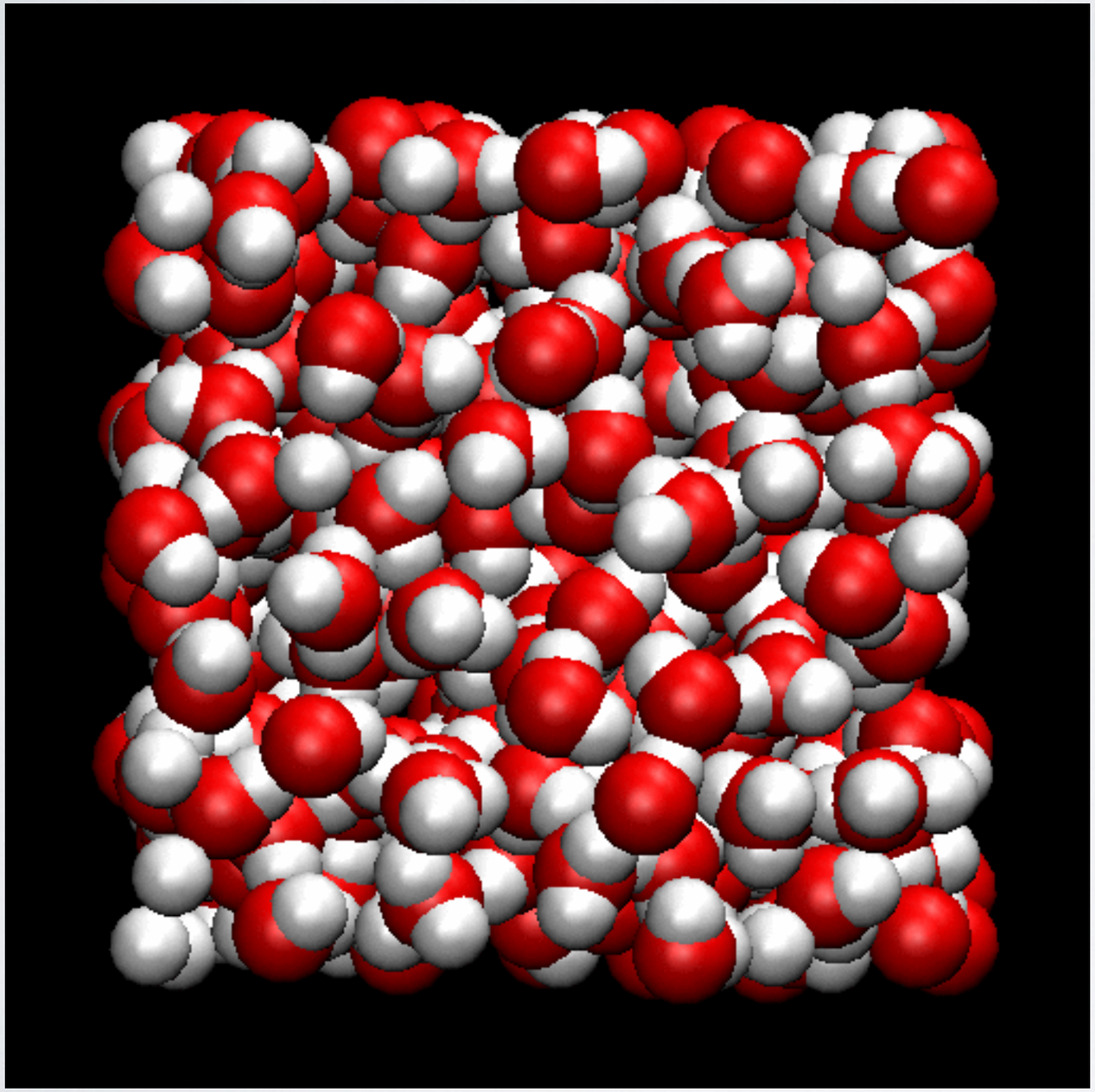

Dynamics of 256 water molecules with in a cibic box with periodic boundary conditions and Ewald summation for the Coulomb forces

SPC/E potential [1]:

- O-O interactions of Lennard-Jones type
- **Coulomb interactions** for O-O,

[1] H. Berendsen, J.R. Grigera, and T.P. Straatsma, J Phys Chem-Us 91, 6269 (1987).

Static site pair correlation functions of water

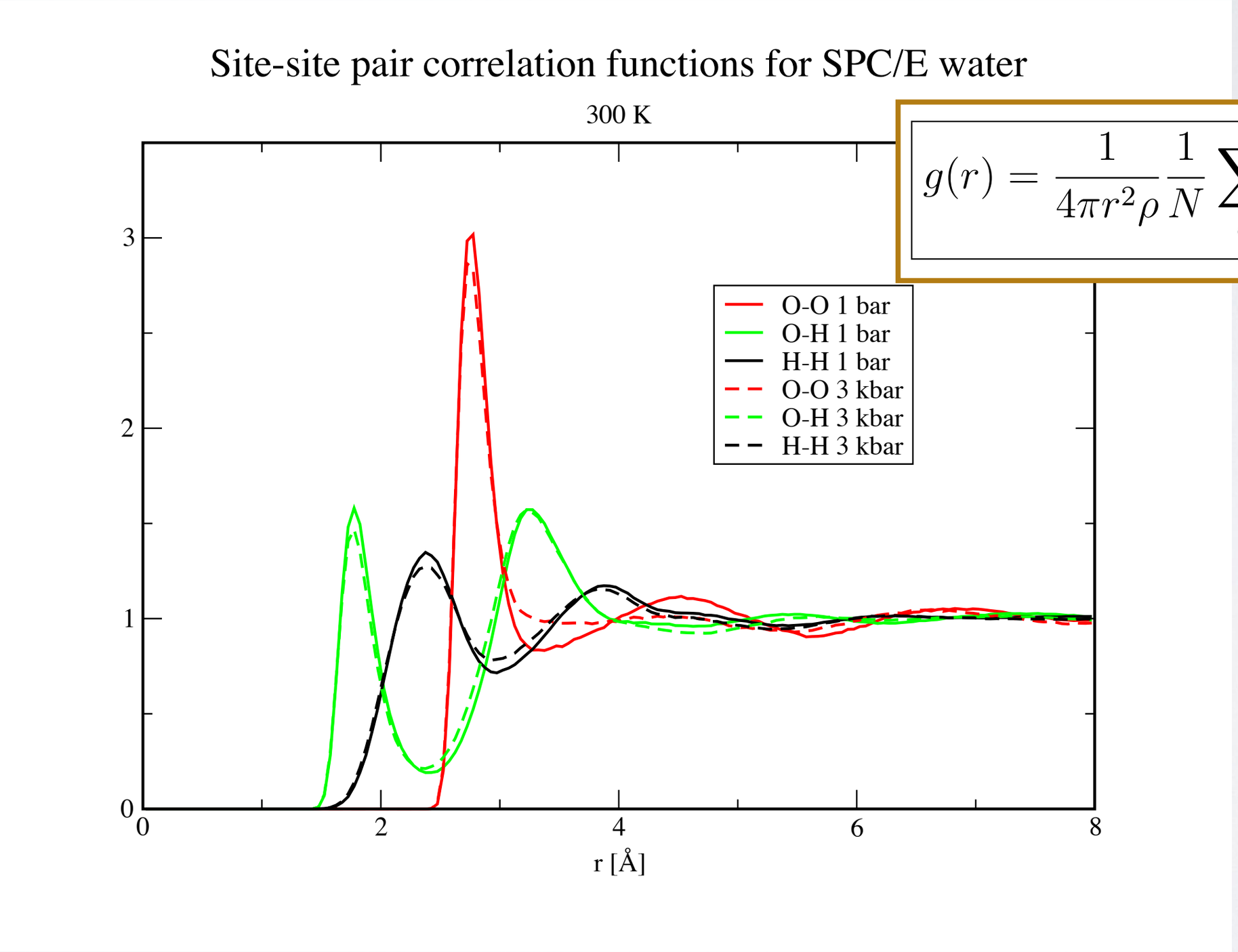

$$g(r) = \frac{1}{4\pi r^2 \rho} \frac{1}{N} \sum_{\alpha} \sum_{\beta \neq \alpha} \langle \delta(r - |R_\alpha - R_\beta|) \rangle$$

Atomic mean square displacements

$$W^{(\alpha)}(n) \approx \frac{1}{N_t - |n|} \sum_{k=0}^{N_t-|n|-1} \left| \mathbf{x}^{(\alpha)}(k+n) - \mathbf{x}^{(\alpha)}(k) \right|^2$$

$$W(n) = \frac{1}{N} \sum_{\alpha=1}^{N} W_{vv}^{(\alpha)}(n)$$ average over molecules

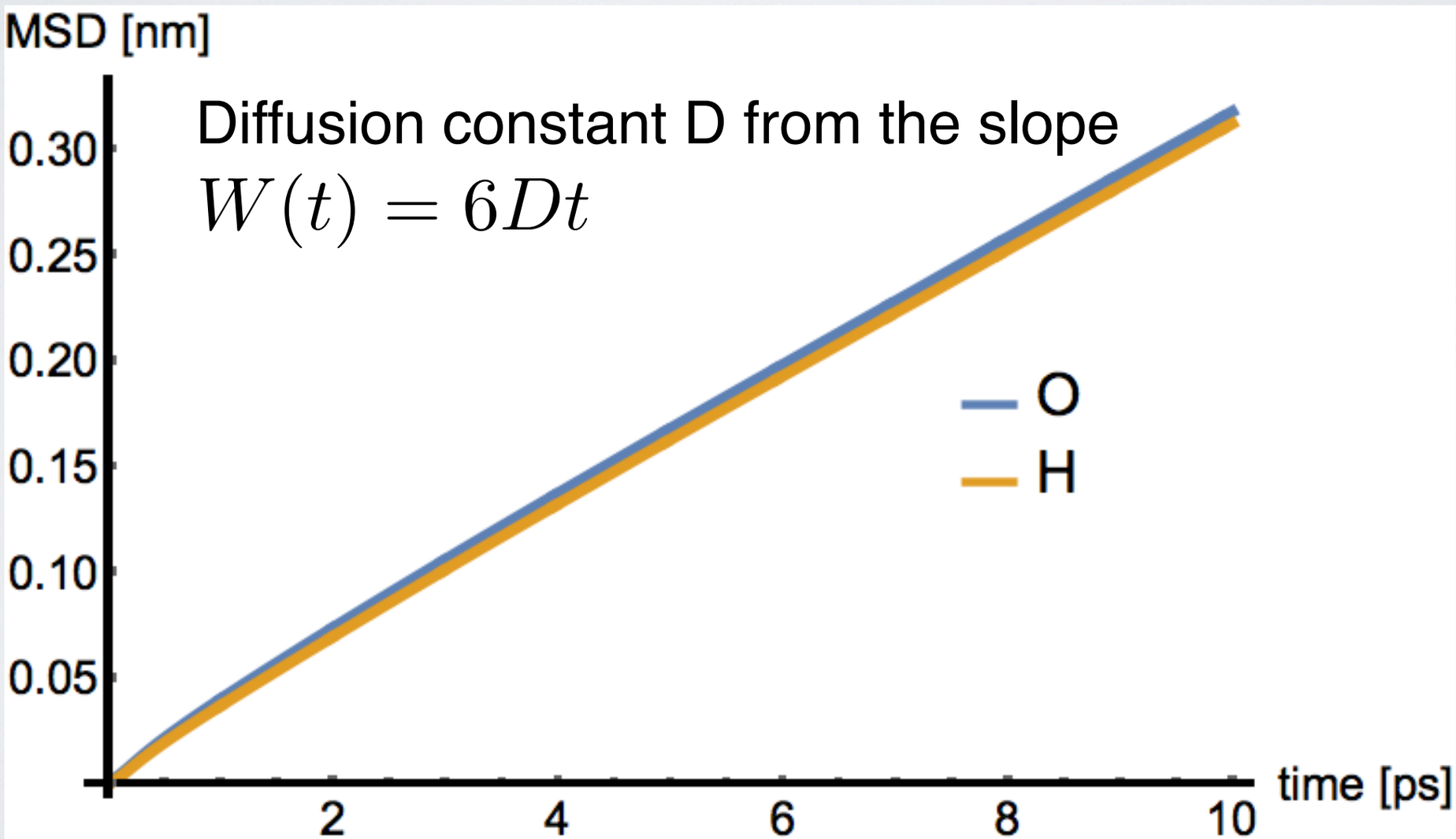

Diffusion constant D from the slope

$$W(t) = 6Dt$$

Remove first jumps due to p.b.c. !

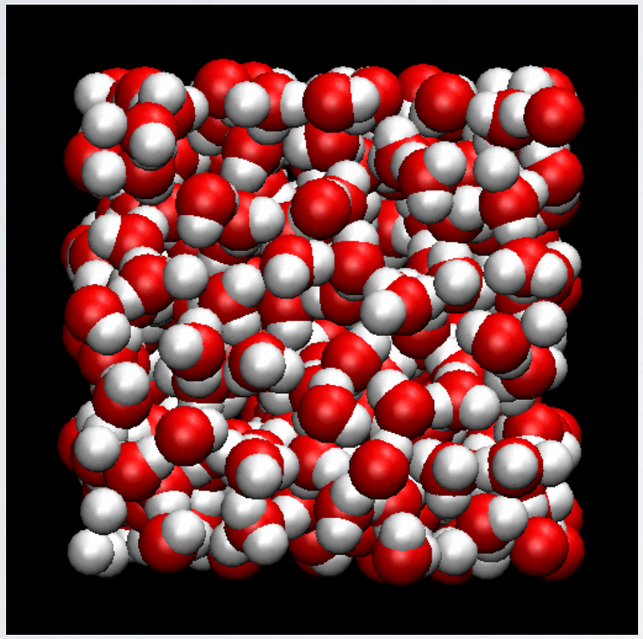

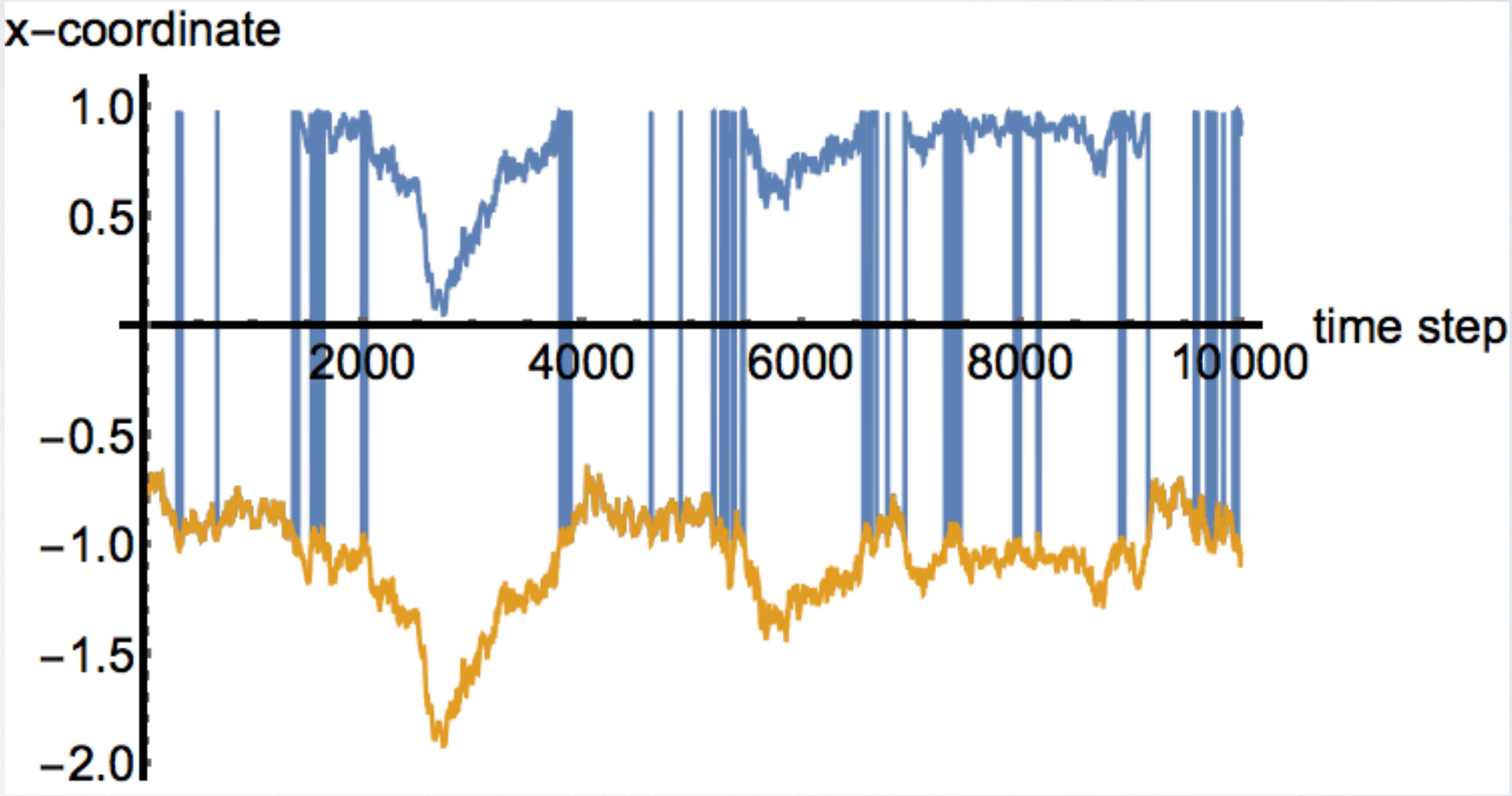

Velocity autocorrelation function (oxygen)

Trajectory

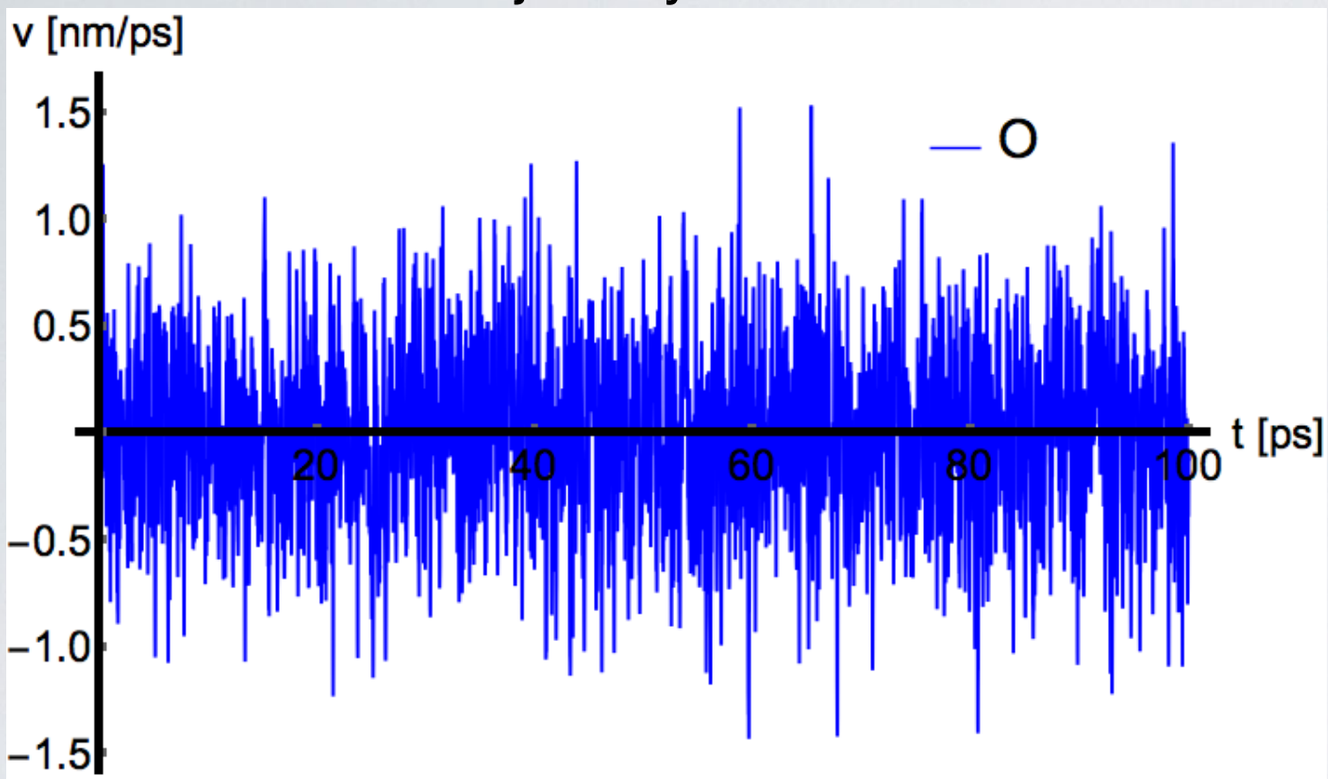

Maxwell distribution

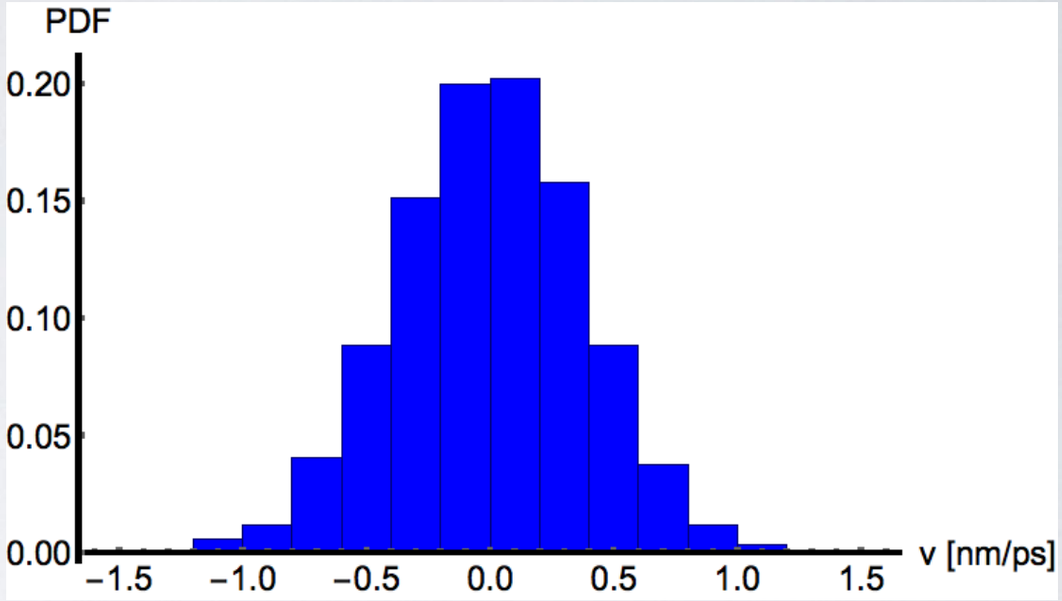

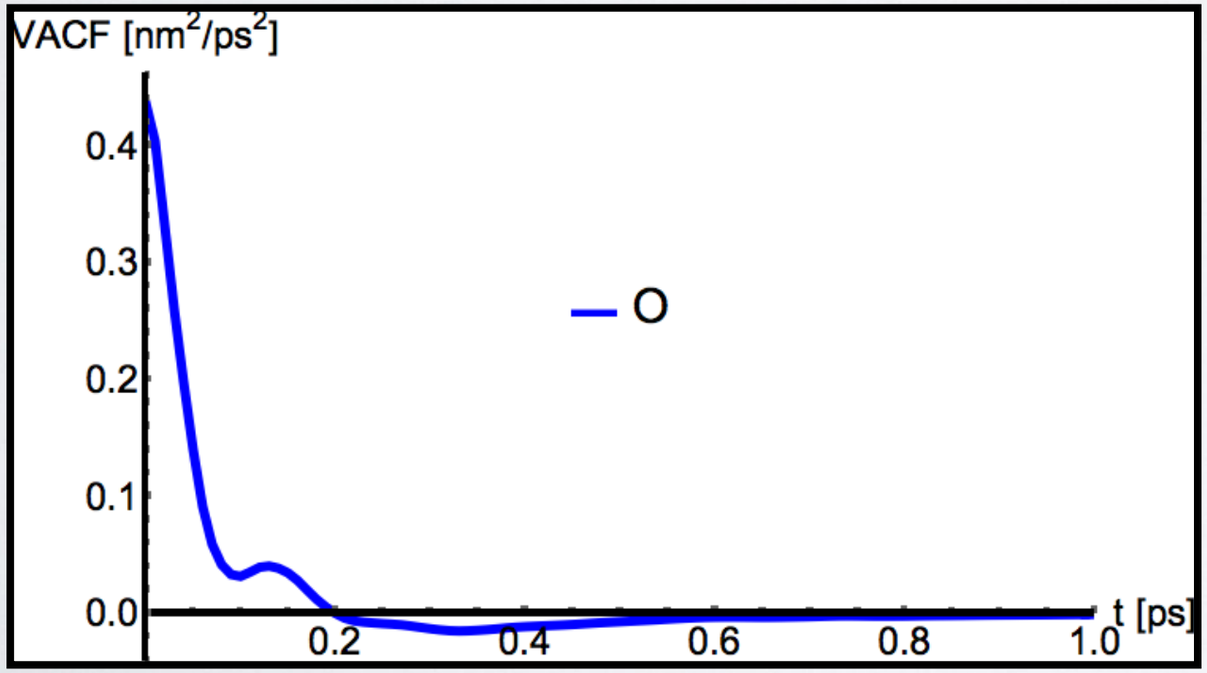

$$c_{vv}^{(\alpha)}(n) \approx \frac{1}{N_t - |n|} \sum_{k=0}^{N_t-|n|-1} \mathbf{v}^{(\alpha)}(k) \cdot \mathbf{v}^{(\alpha)}(k+n)$$

$$c_{vv}(n) = \frac{1}{N} \sum_{\alpha=1}^{N} c_{vv}^{(\alpha)}(n)$$

average over molecules

Velocity autocorrelation function (hydrogen)

Trajectory

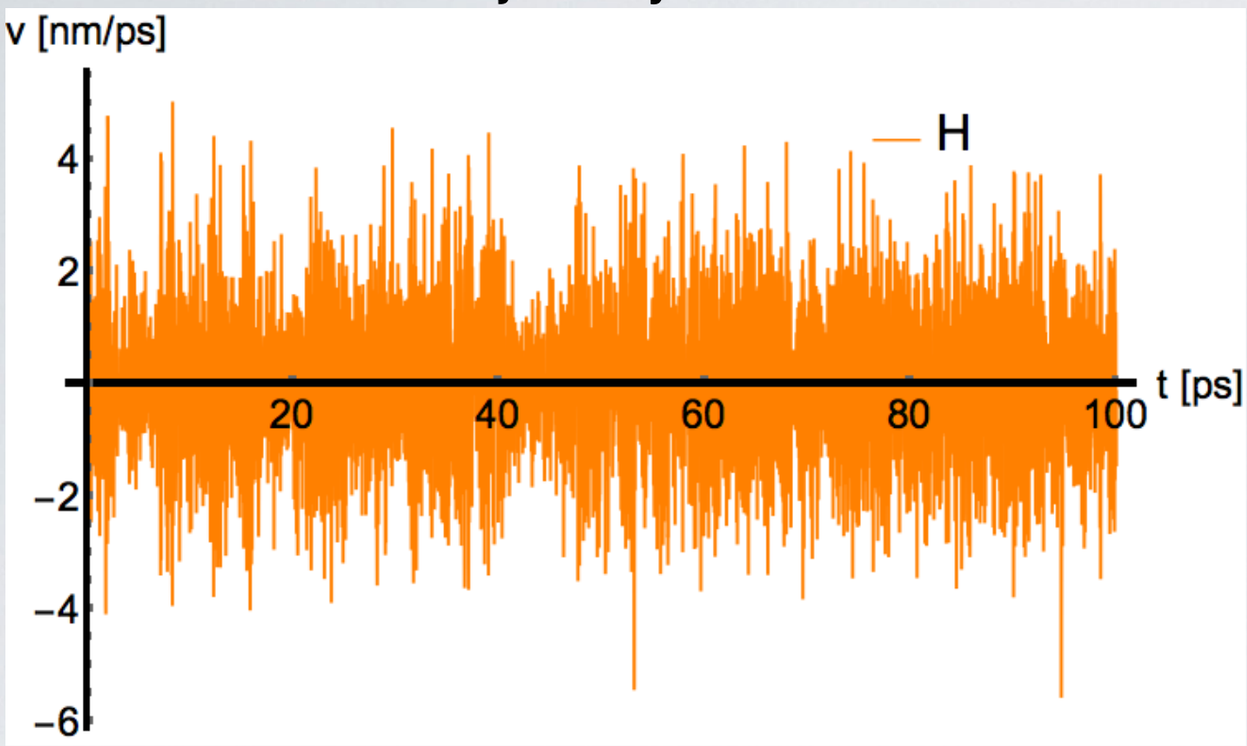

Maxwell distribution

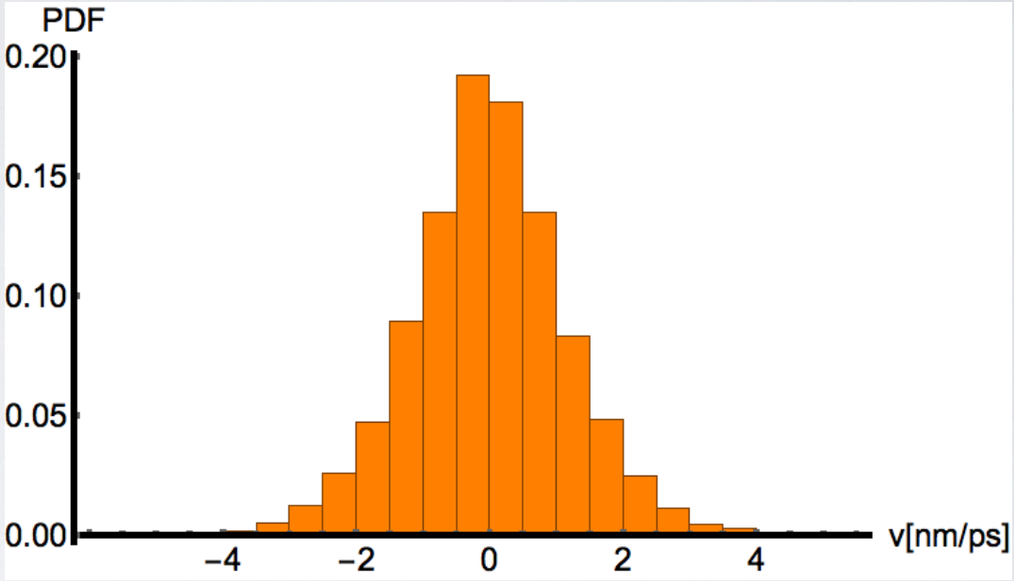

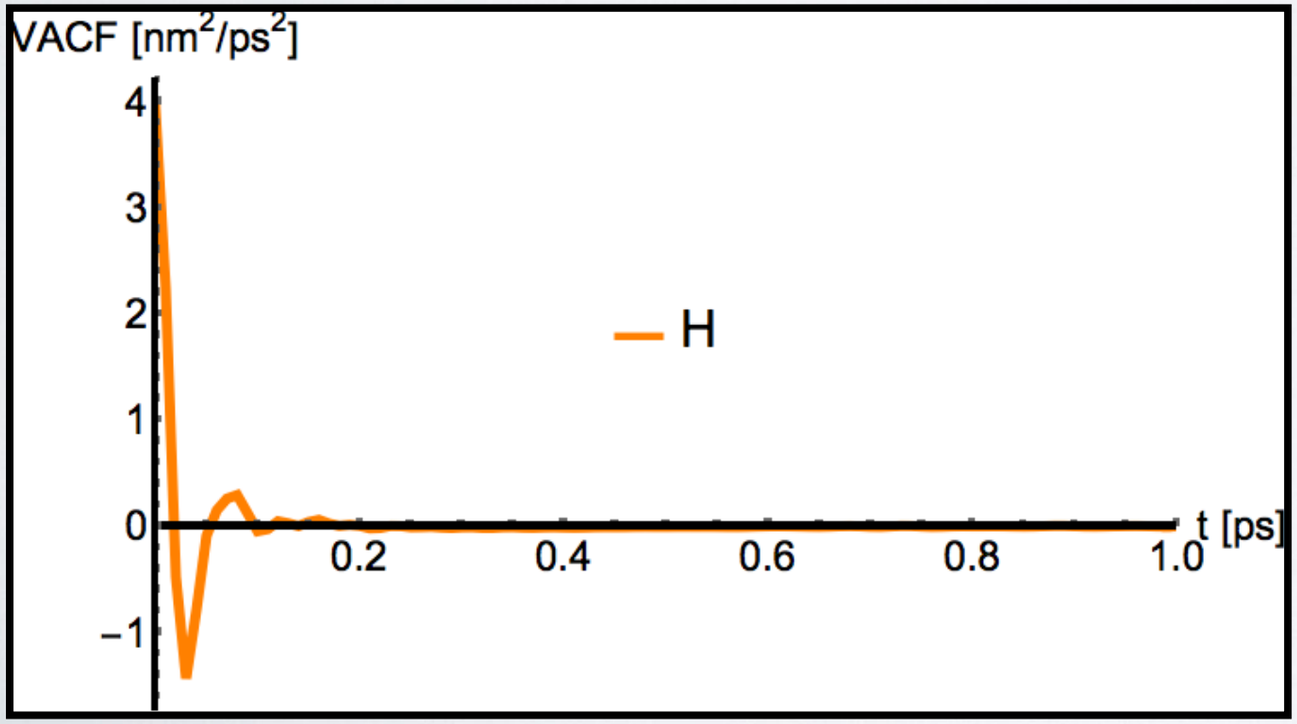

Density of States, VACF, and diffusion coefficient

$$g(\omega) \equiv \int_0^\infty dt \, \cos \omega t \, c_{vv}(t).$$

$$D = \int_0^\infty dt \, c_{vv}(t) = g(0),$$

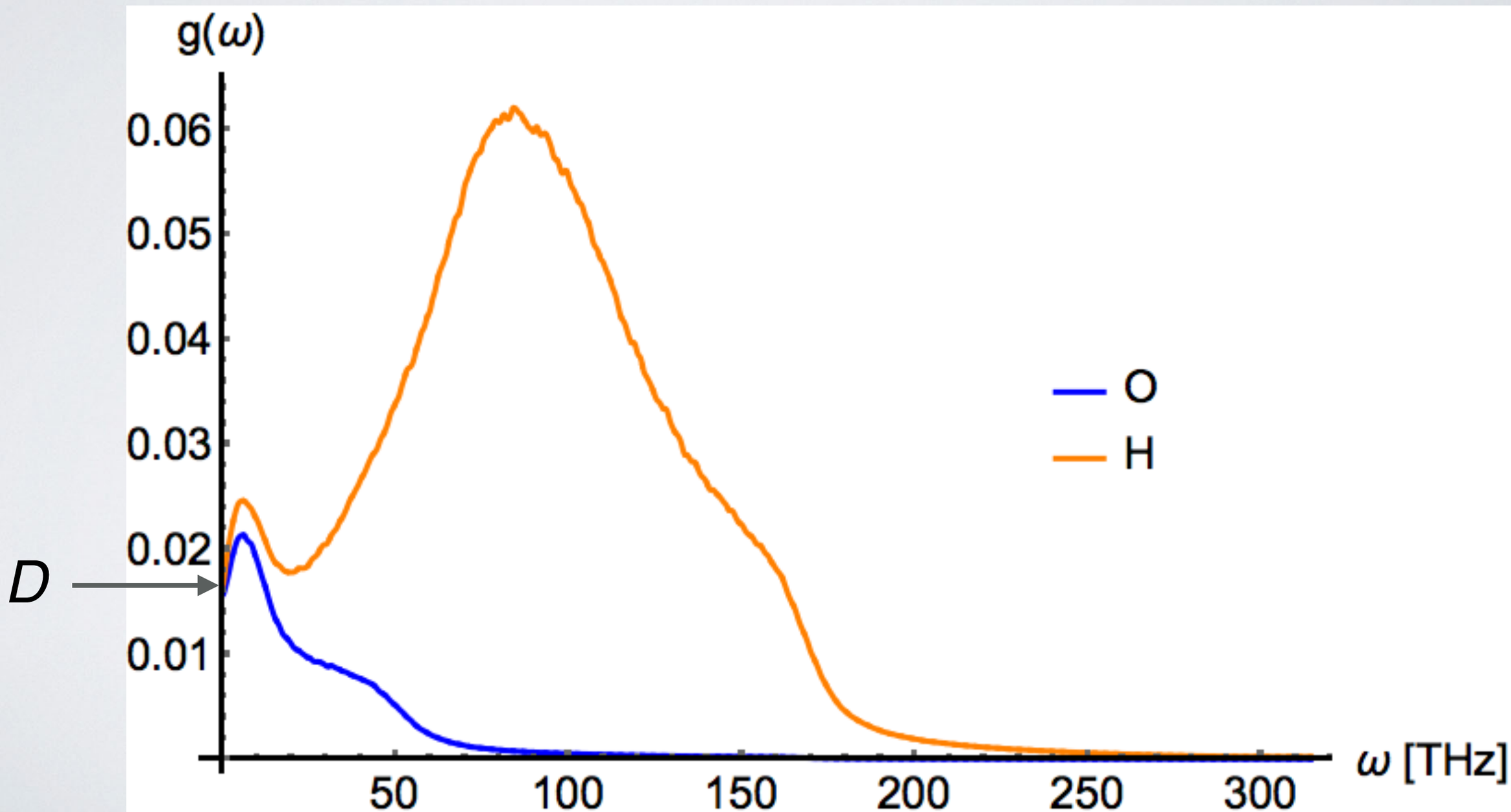

Using computer simulations to understand “real” experiments

An example from biophysics : interpreting quasielastic neutron scattering from proteins to understand their dynamics

Thermal neutron scattering

Exploring the structural dynamics of condensed matter on the atomic scale (0.1-10 nm, sub ps - 10 ns)

Setup for a neutron scattering experiment

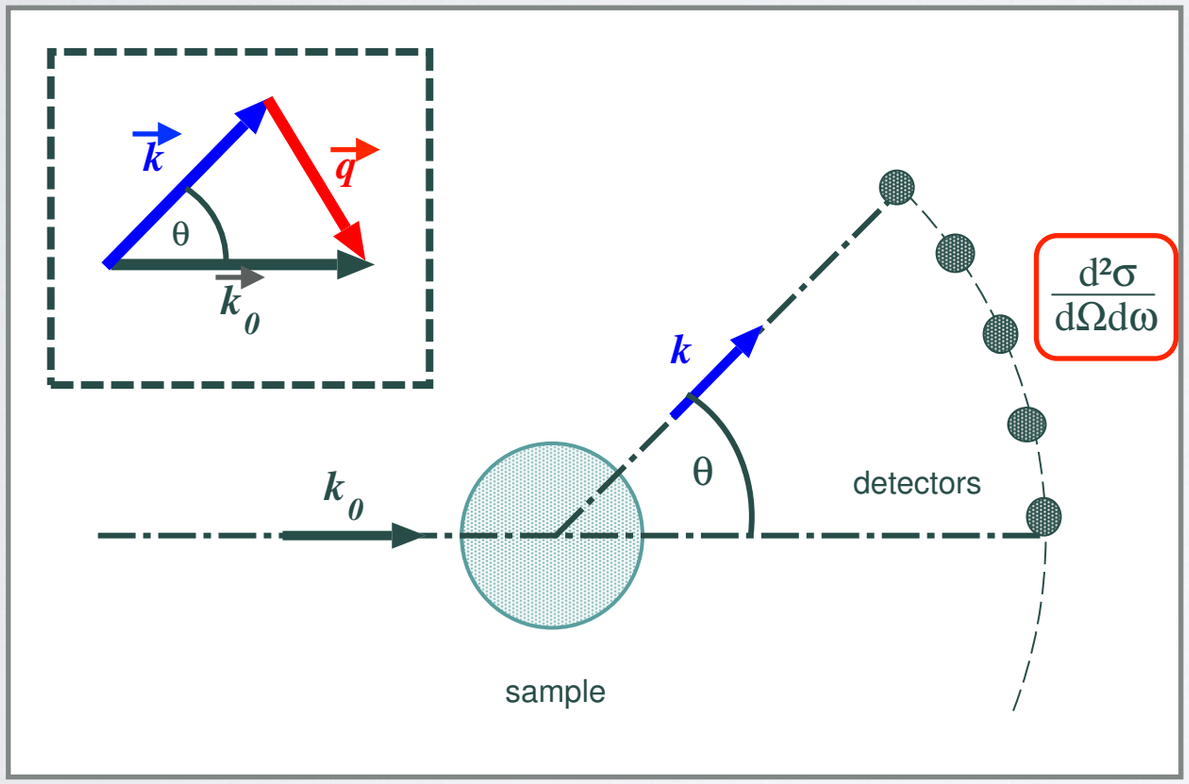

Energy spectrum

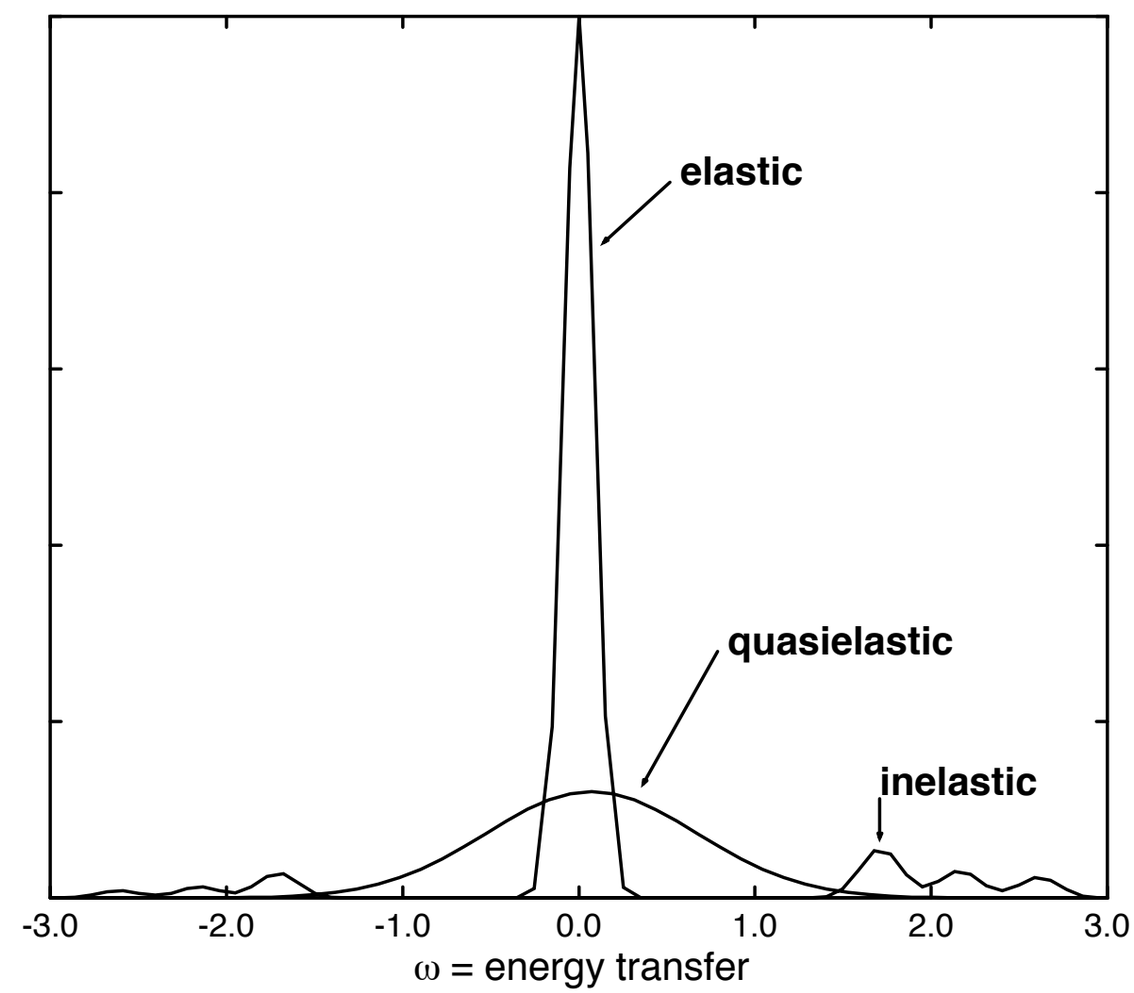

Momentum transfer:
$\mathbf{q} = \mathbf{k}_0 - \mathbf{k} = (\mathbf{p}_0 - \mathbf{p})/\hbar$

Energy transfer:
$\omega = (E_0 - E)/\hbar$

Differential scattering cross section

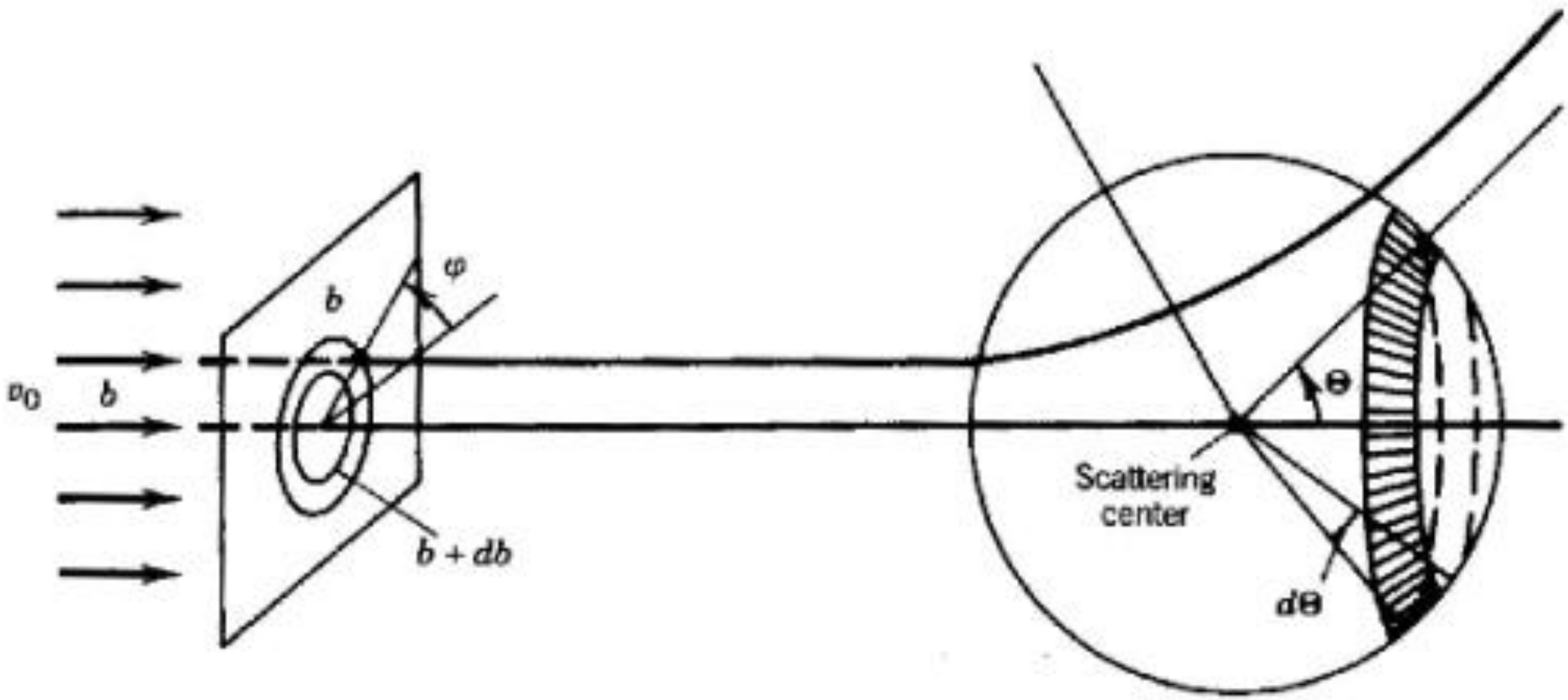

Figure 1-2-5. Relation between the impact parameter b and the CM scattering angle Θ for the one-particle equivalent problem of a purely repulsive Coulomb potential $V_{coul}(r)$. The outer circle in the plane at the left corresponds to the values b and Θ, the inner circle to the values $b - |db|$ and $\Theta + |d\Theta|$. [Adapted from Goldstein (1980).]

Wave length of thermal neutrons

Using the De Broglie relations[2]

$$\vec{p} = \hbar\vec{k}, \qquad |\vec{k}| = \frac{2\pi}{\lambda},$$

one finds for $E = \vec{p}^{\,2}/2m = k_B T$ et $T = 300\,\mathrm{K}$ a wavelength of

$$\lambda = 1.778\,\text{Å}.$$

The wave length is this compatible with typical interatomic distances between the atoms in condensed matter systems. Since $E \approx k_B T$ is comparable with their energy, thermal neutron scattering is a unique tool for studying the structure and the dynamics of condensed matter.

[2] $\hbar = h/(2\pi) = 1.05457 \times 10^{34}$ Js is the reduced Planck constant.

Interaction of neutrons with matter

Neutrons interact with matter primarily through a short-ranged (fm) neutron-nucleus interaction, which is described through Fermi's pseudo-potential,

$$T = \frac{2\pi\hbar^2}{m} b\,\delta(\vec{r} - \vec{R}).$$

Here $\vec{r}$ and $\vec{R}$ is, respectively, the position operator of the neutron and the nucleaus of the scattering atom and the (generally complex) scattering length b takes values in the fm range. It depends on the relative orientation of the neutron and the nuclear spin. The symbol m denotes the neutron mass. The scattering cross section of a fixed atom is

$$\sigma = 4\pi|b|^2.$$

The (normalized) differential scattering cross section for N scattering atoms and an unpolarized neutron beam/sample is

$$\boxed{\frac{d^2\sigma}{d\Omega d\omega} = \frac{|\vec{k}|}{|\vec{k}_0|}\frac{1}{2\pi\hbar}\int_{-\infty}^{+\infty} dt\, e^{-i\omega t}\frac{1}{N}\sum_{\alpha=1}^{N}\sum_{\beta=1}^{N}\overline{b_\alpha^* b_\beta}\left\langle e^{-i\vec{q}\cdot\vec{R}_\alpha(0)}e^{i\vec{q}\cdot\vec{R}_\beta(t)}\right\rangle}$$

where

$$\boxed{\langle A(0)B(t)\rangle = \frac{1}{Z}\mathrm{tr}\left\{Ae^{iHt/\hbar}Be^{-iHt/\hbar}\right\}}$$

denotes a quantum time correlation function. Here H is the Hamilton operator of the scattering system and $Z = \mathrm{tr}\{e^{-\beta H}\}$ is the partition function, with $\beta = (k_B T)^{-1}$. The overline denotes an average over relative neutron-nucleus spin orientations. The incident and scattered neutron have the momenta $\hbar\vec{k}_0$ and $\hbar\vec{k}$, respectively.

Dynamic structure factor

$$\frac{d^2\sigma}{d\Omega d\omega} = \frac{|\vec{k}|}{|\vec{k}_0|}\mathcal{S}(\vec{q},\omega)$$

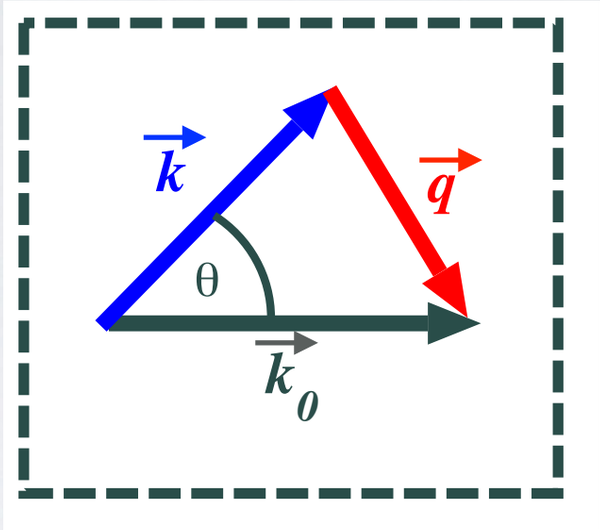

$$\mathcal{S}(\vec{q},\omega) = \frac{1}{2\pi\hbar}\int_{-\infty}^{+\infty} dt\, e^{-i\omega t}\mathcal{I}(\vec{q},t)$$

Dynamic structure factor

$$\mathcal{I}(\vec{q},t) = \frac{1}{N}\sum_{\alpha=1}^{N}\sum_{\beta=1}^{N}\overline{b_\alpha^* b_\beta}\left\langle e^{-i\vec{q}\cdot\vec{R}_\alpha(0)}e^{i\vec{q}\cdot\vec{R}_\beta(t)}\right\rangle$$

Intermediate scattering function

Coherent and incoherent scattering

The intermediate scattering function is split into a coherent part, reflecting collective motions, and and incoherent part, reflecting single particle motions,

$$\boxed{\mathcal{I}(\vec{q},t) = \mathcal{I}_{\text{coh}}(\vec{q},t) + \mathcal{I}_{\text{inc}}(\vec{q},t)}$$

Defining $b_{\alpha\,\text{coh}} = \overline{b_\alpha}$ and $b_{\alpha\,\text{inc}} = \sqrt{\overline{|b_\alpha|^2} - \left|\overline{b_\alpha}\right|^2}$, one has

$$\boxed{\begin{aligned} \mathcal{I}_{\text{coh}}(\vec{q},t) &= \frac{1}{N}\sum_{\alpha=1}^{N}\sum_{\beta=1}^{N} b^*_{\alpha\,\text{coh}}\, b_{\beta\,\text{coh}} \left\langle e^{-i\vec{q}\cdot\vec{R}_\alpha(0)} e^{i\vec{q}\cdot\vec{R}_\beta(t)} \right\rangle \\ \mathcal{I}_{\text{inc}}(\vec{q},t) &= \frac{1}{N}\sum_{\alpha=1}^{N} |b_{\alpha\,\text{inc}}|^2 \left\langle e^{-i\vec{q}\cdot\vec{R}_\alpha(0)} e^{i\vec{q}\cdot\vec{R}_\alpha(t)} \right\rangle \end{aligned}}$$

Understand the dynamics of proteins

Nature Vol. 280 16 August 1979

Temperature-dependent X-ray diffraction as a probe of protein structural dynamics

Hans Frauenfelder, Gregory A. Petsko* & Demetrius Tsernoglou
Department of Physics, University of Illinois at Urbana-Champaign, Urbana, Illinois 61801
and
Department of Biochemistry, Wayne State University School of Medicine, Detroit, Michigan 48201

proteins have *dynamic* structures

Myoglobin

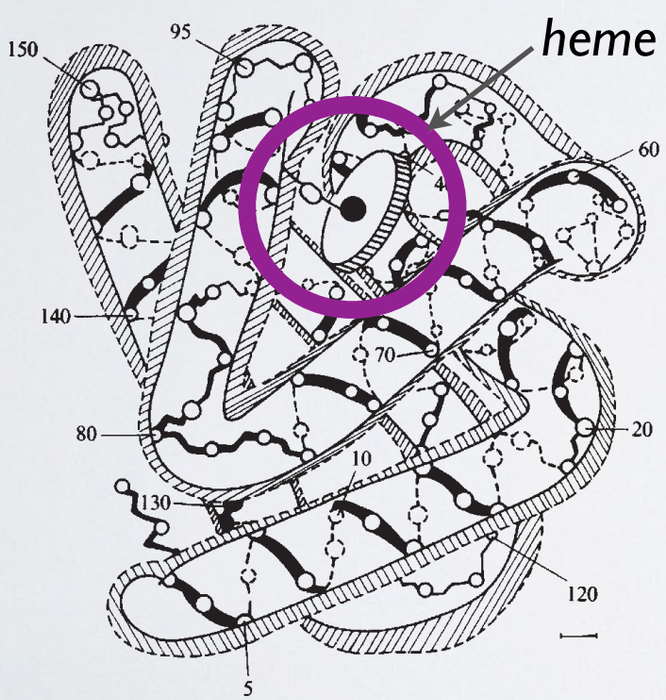

Fig. 3 Backbone (main chain) structure of myoglobin. The solid lines indicate the static structure as given in ref. 37. Circles denote the C^{α} carbons; some residue numbers are given. The shaded area gives the region reached by conformational substates with a 99% probability. Scale bar, 2 Å.

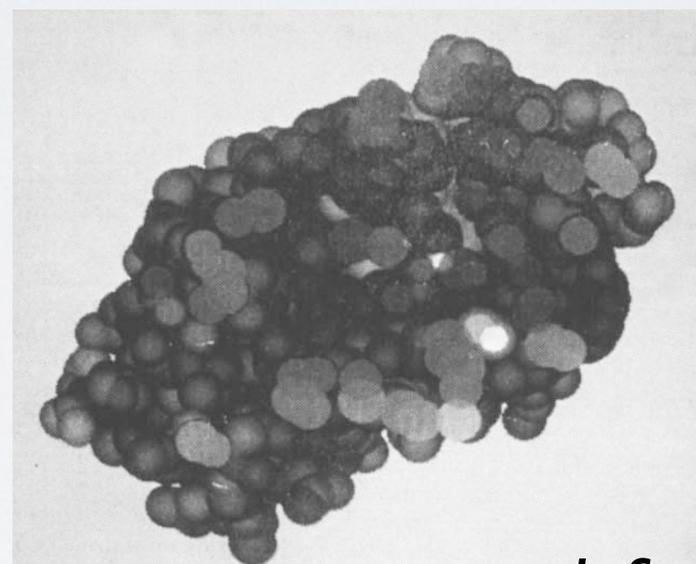

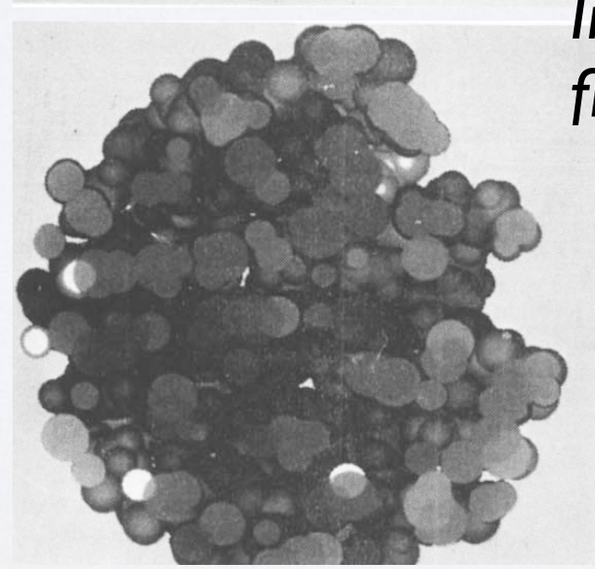

Inferring atomic motions from crystallgraphic B-factors

Conformational substates in a protein: Structure and dynamics of metmyoglobin at 80 K

(low-temperature crystallography/Mössbauer absorption/Debye–Waller factor/intramolecular motion/lattice disorder)

H. Hartmann*, F. Parak*§, W. Steigemann*, G. A. Petsko†, D. Ringe Ponzi†, and H. Frauenfelder‡

Proc. Natl. Acad. Sci. USA
Vol. 79, pp. 4967–4971, August 1982
Biophysics

Protein dynamical transition

Average position fluctuations per residue from ***crystallography*** *at 80 K and 300 K*

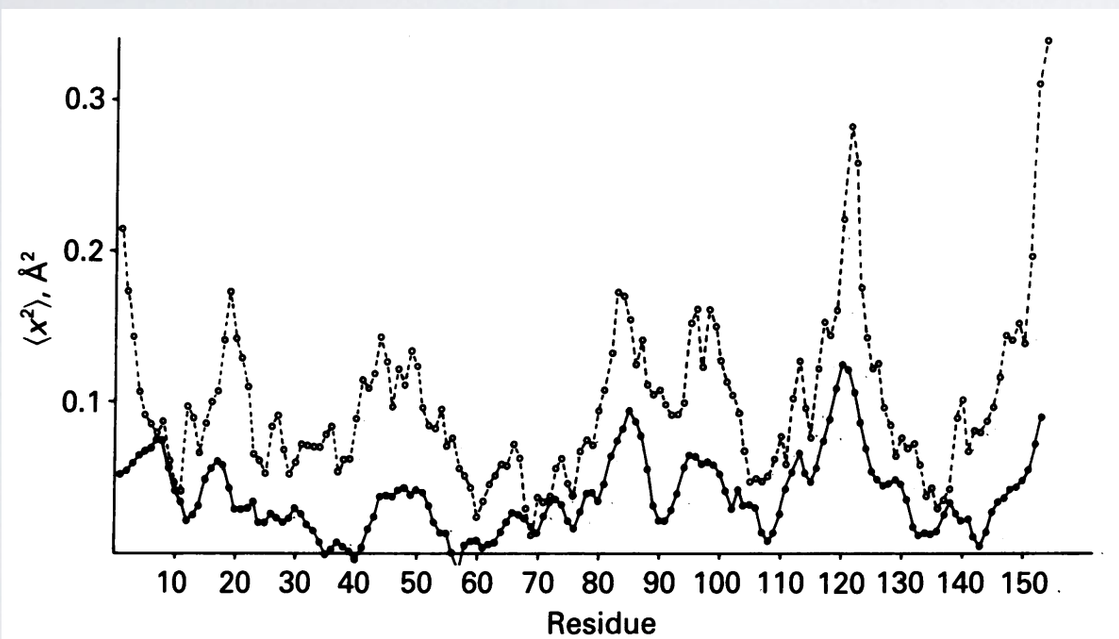

Position fluctuation of the Fe atom from ***Mössbauer spectroscopy***

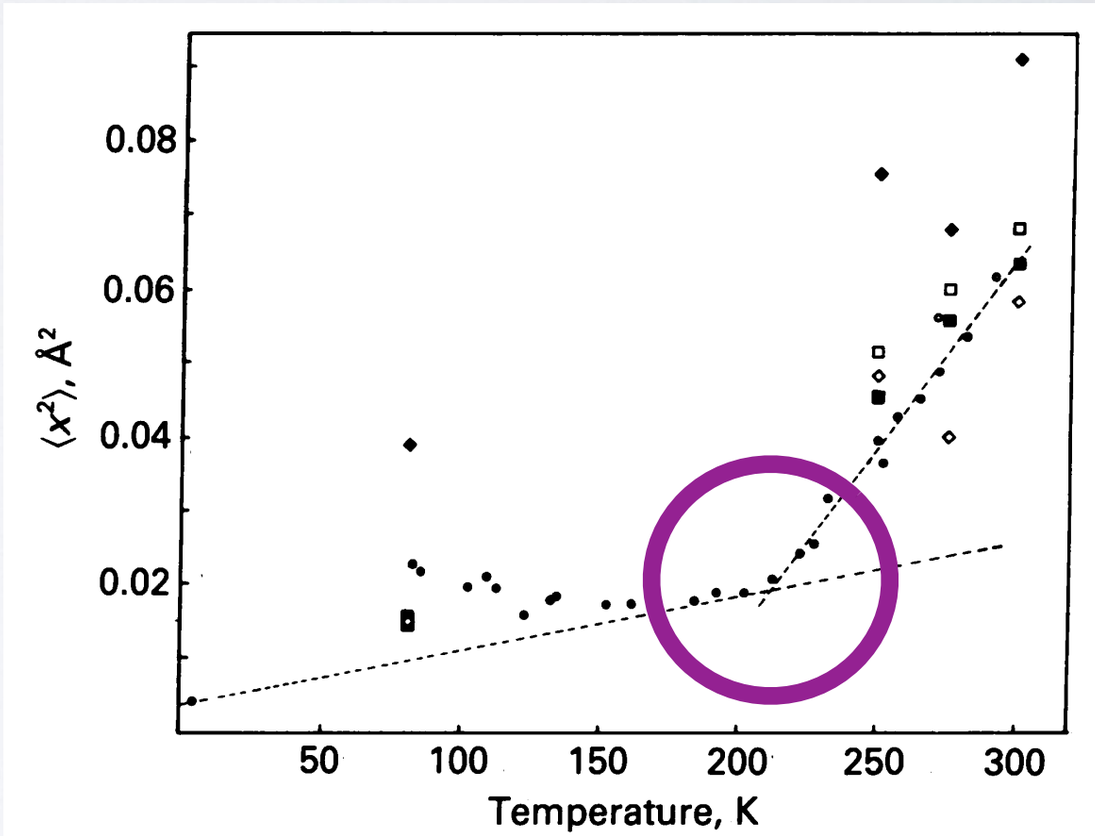

FIG. 3. Temperature dependence of $\langle x^2 \rangle$ values. ●, Fe measured by Mössbauer spectroscopy (13); ■, Fe determined by x-ray analysis; ◆, histidine-93(F8); ◇, histidine-64(E7).

Dynamical transition of myoglobin revealed by inelastic neutron scattering

Wolfgang Doster*, Stephen Cusack† & Winfried Petry‡

NATURE VOL. 337 23 FEBRUARY 1989

Dynamical transition by neutron scattering

Elastic scattering

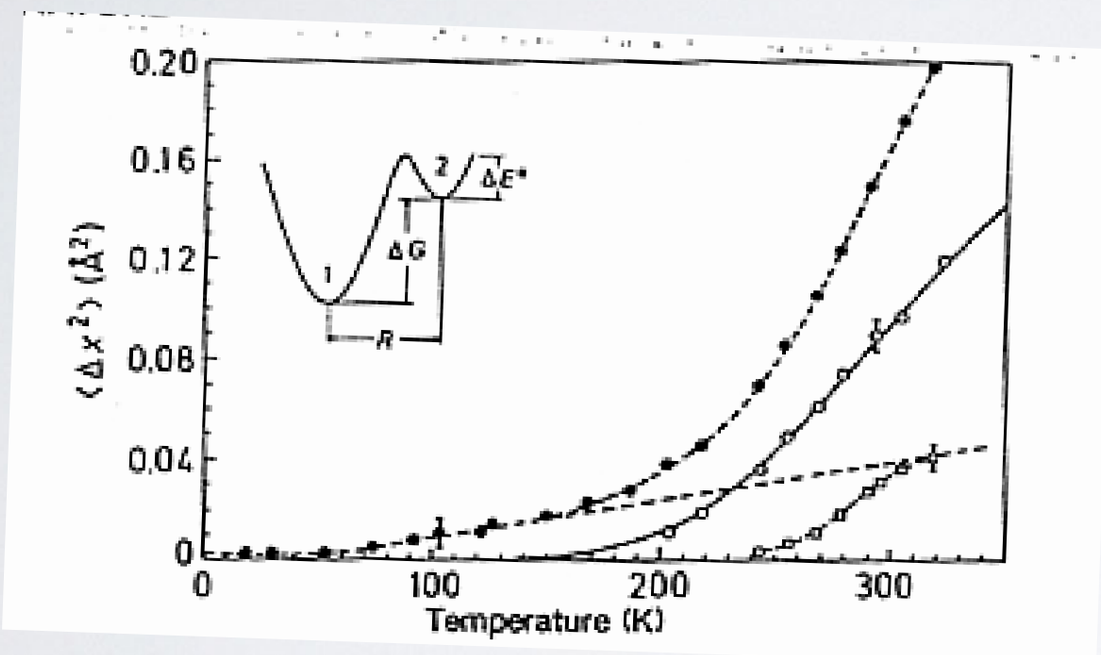

Position fluctuation averaged over <u>all</u> (hydrogen) atoms

Quasielastic scattering

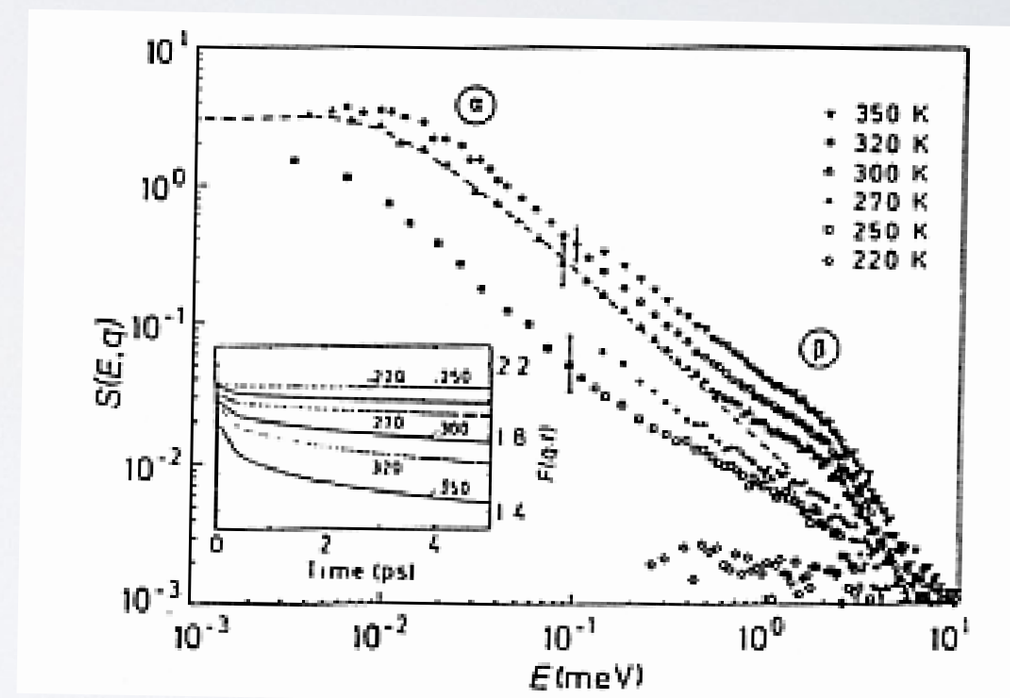

Onset of diffusive motions on the picosecond time scale

The protein side chain “liquid”

J. Mol. Biol. (1994) **242**, 181–185

COMMUNICATION

Liquid-like Side-chain Dynamics in Myoglobin

Gerald R. Kneller[1,2] and Jeremy C. Smith[2]

[1]*IBM France*
68–76 Quai de la Rapée F-75012 Paris, France

[2]*SBPM DBCM*
Commissariat à l'Energie Atomique, CE Saclay F-91191 Gif-sur-Yvette, France

At temperatures above ~200 K the motions of atoms in globular proteins contain a non-vibrational component that gives rise to characteristic elastic and quasi-elastic neutron scattering profiles. There is evidence that the non-vibrational dynamics is required for protein function. Here we show by analysing a molecular dynamics simulation of myoglobin that the neutron scattering results from liquid-like rigid-body motion of the protein side-chains.

Keywords: protein dynamics; neutron scattering; molecular dynamics; myoglobin

Force field for biomolecular simulations

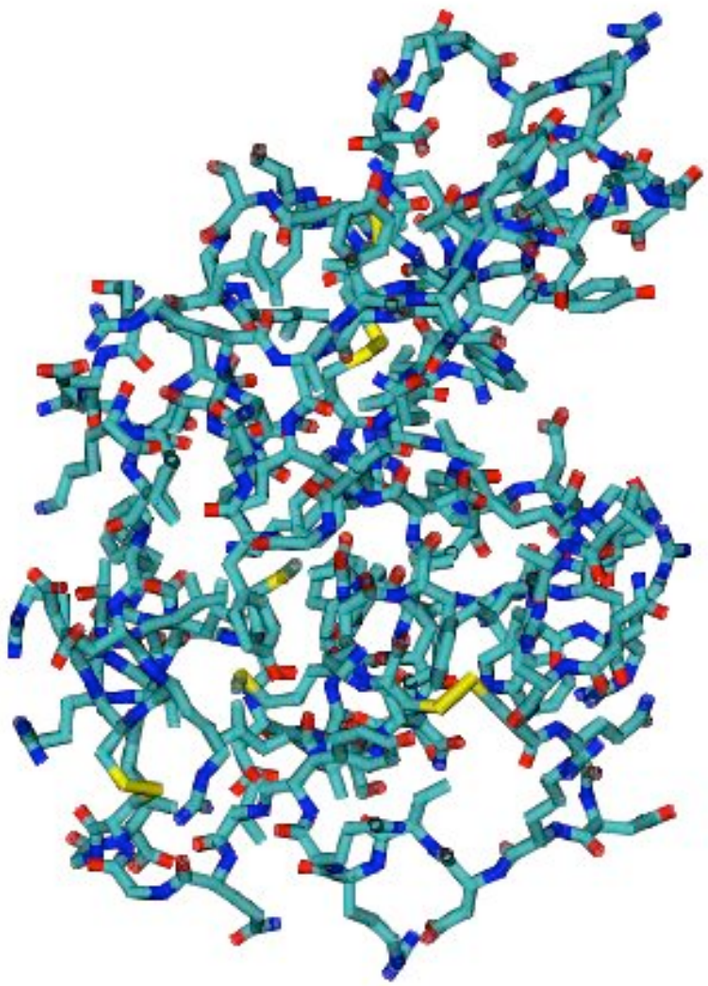

Lysozyme

$$U = \sum_{\text{bonds } ij} k_{ij}(r_{ij} - r_{ij}^{(0)})^2 + \sum_{\text{angles } ijk} k_{ijk}(\phi_{ijk} - \phi_{ijk}^{(0)})^2$$

$$+ \sum_{\text{dihedrals } ijkl} k_{ijkl}\cos(n_{ijkl}\theta_{ijkl} - \delta_{ijkl})$$

$$\left.\begin{aligned} &+ \sum_{\text{all pairs } ij} 4\epsilon_{ij}\left(\frac{\sigma_{ij}^{12}}{r^{12}} - \frac{\sigma_{ij}^{6}}{r^{6}}\right) \\ &+ \sum_{\text{all pairs } ij} \frac{q_i q_j}{4\pi\epsilon_0 r_{ij}} \end{aligned}\right\} \text{non-bonded.}$$

The force field (Amber)

Simulated motions in myoglobin

J. Mol. Biol. (1994) **242**, 181–185

COMMUNICATION

Liquid-like Side-chain Dynamics in Myoglobin

Gerald R. Kneller[1,2] and Jeremy C. Smith[2]

Backbone

The "side-chain liquid"

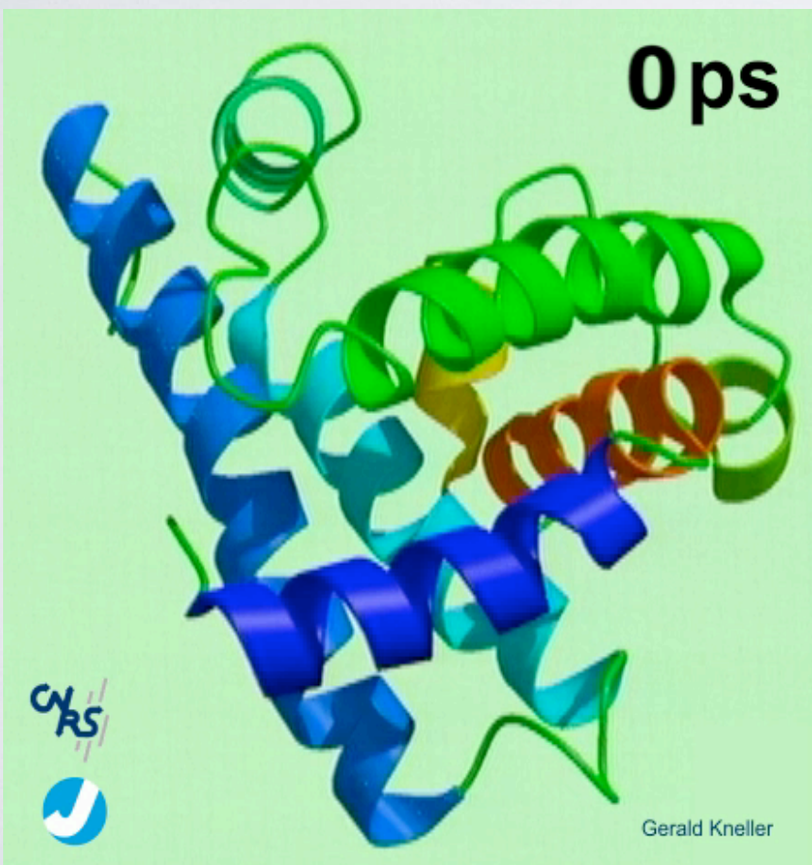

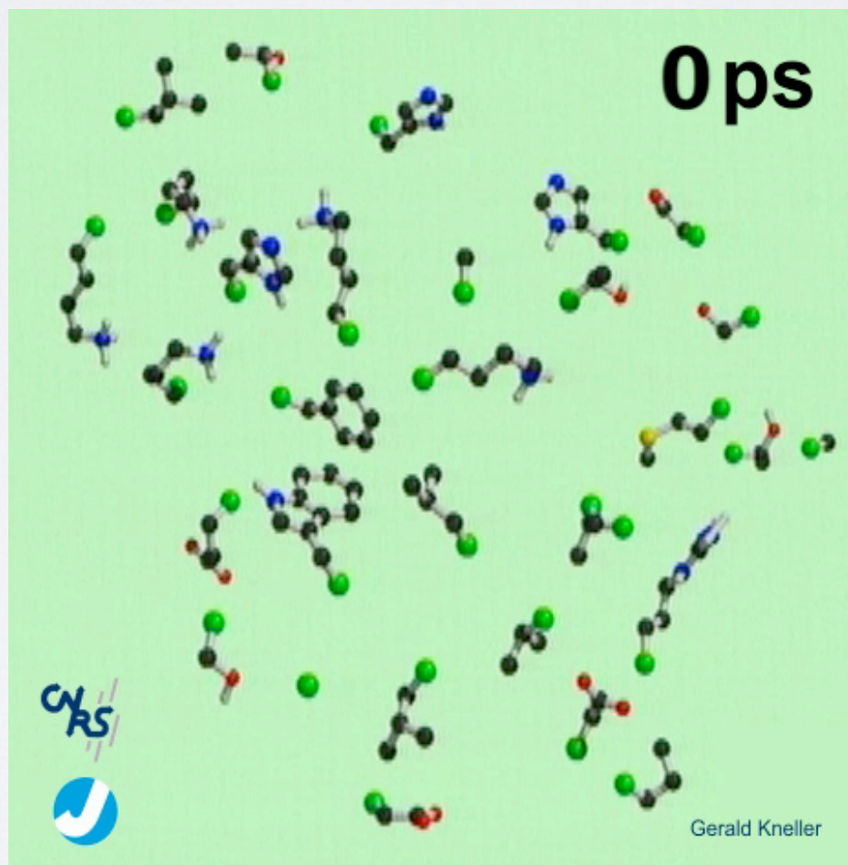

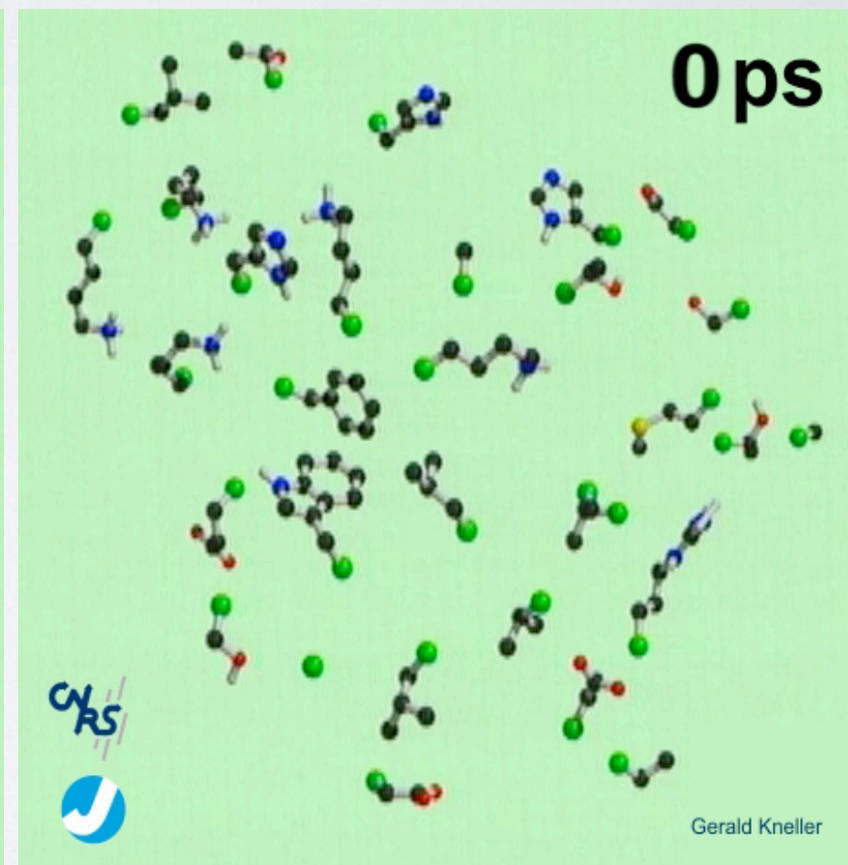

flexible

rigid

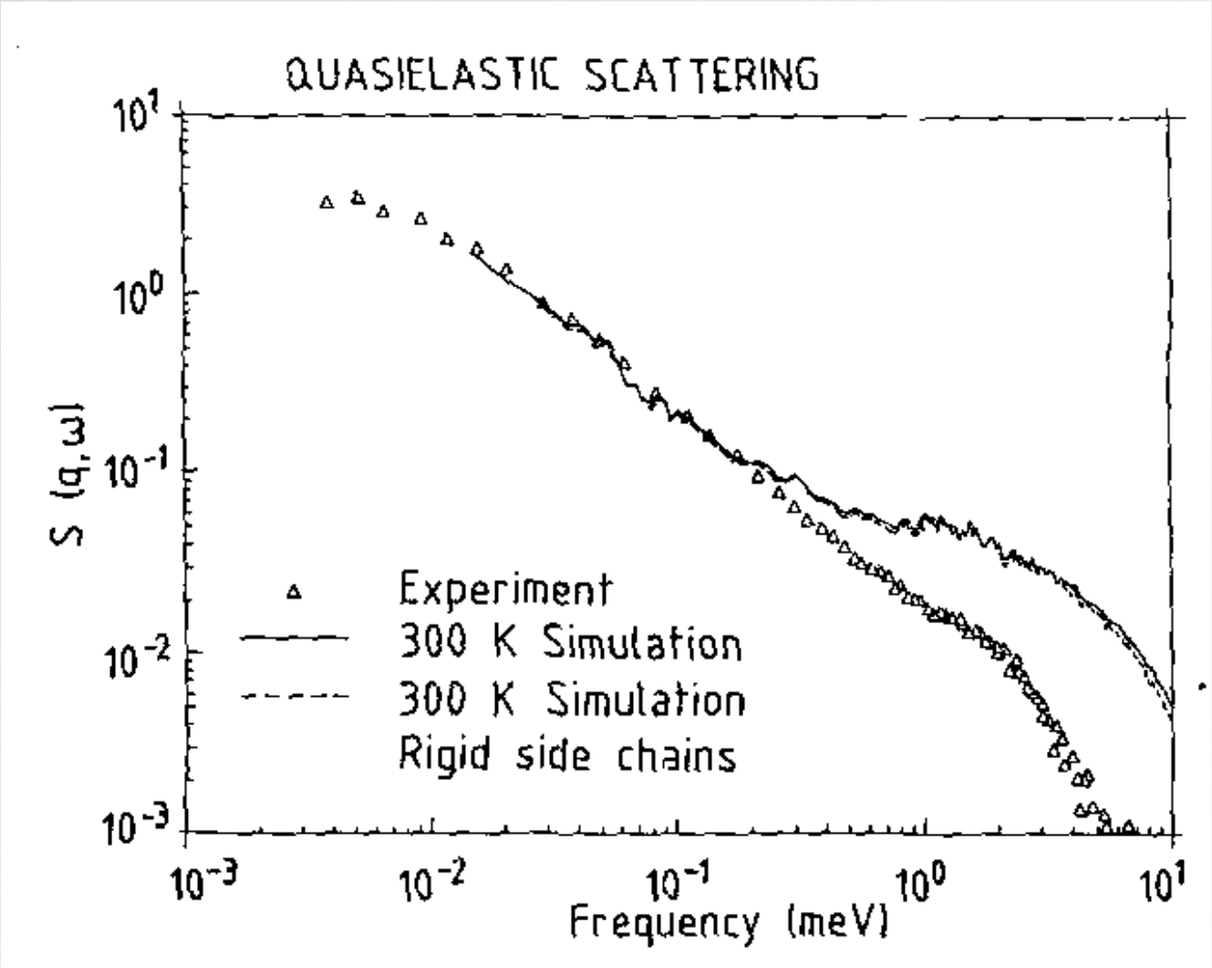
QUASIELASTIC SCATTERING
S (q,ω)
Frequency (meV)
Experiment
300 K Simulation
300 K Simulation
Rigid side chains

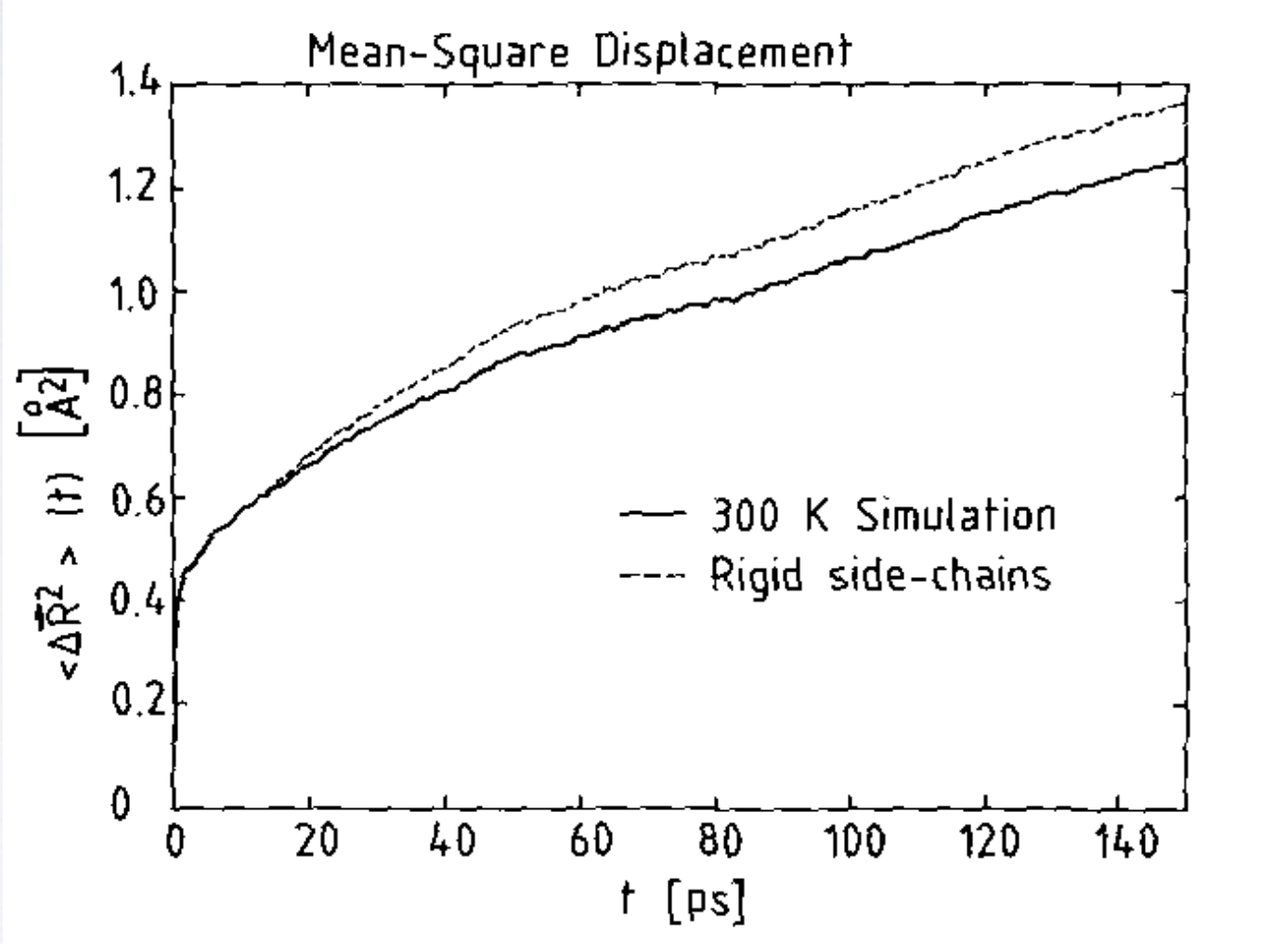
Mean-Square Displacement
<ΔR² > (t) [Å²]
t [ps]
300 K Simulation
Rigid side-chains

Software for interfering MD simulations and neutron scattering experiments

nMoldyn

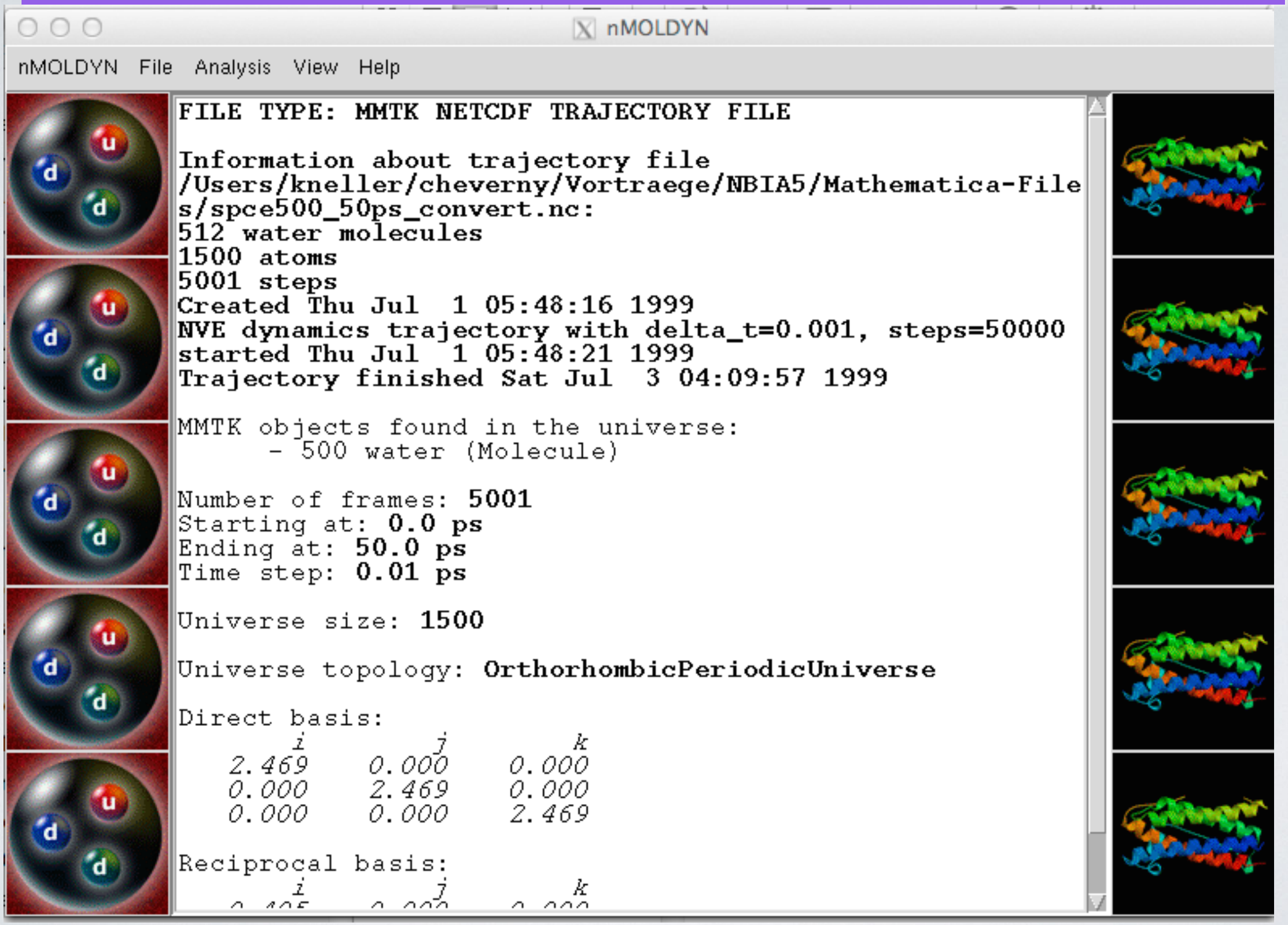
nMOLDYN
nMOLDYN File Analysis View Help
FILE TYPE: MMTK NETCDF TRAJECTORY FILE
Information about trajectory file
/Users/kneller/cheverny/Vortraege/NBIA5/Mathematica-File
s/spce500_50ps_convert.nc:
512 water molecules
1500 atoms
5001 steps
Created Thu Jul 1 05:48:16 1999
NVE dynamics trajectory with delta_t=0.001, steps=50000
started Thu Jul 1 05:48:21 1999
Trajectory finished Sat Jul 3 04:09:57 1999
MMTK objects found in the universe:
- 500 water (Molecule)
Number of frames: 5001
Starting at: 0.0 ps
Ending at: 50.0 ps
Time step: 0.01 ps
Universe size: 1500
Universe topology: OrthorhombicPeriodicUniverse
Direct basis:
i j k
2.469 0.000 0.000
0.000 2.469 0.000
0.000 0.000 2.469
Reciprocal basis:
i j k

Ideal and «real» *in silico* experiments...

Integrating molecular simulation in "virtual" experiments probing the structure and dynamics of condensed matter

Model | **Simulation** | **Ideal experiment** | **Real experiment**

$$F(q,t) = E_\alpha(-[t/\tau(q)]^\alpha)$$

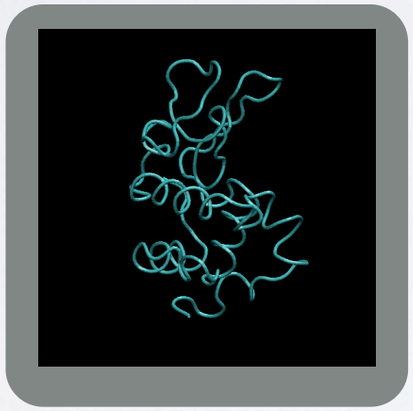

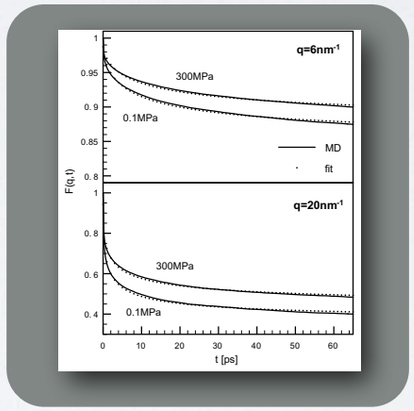

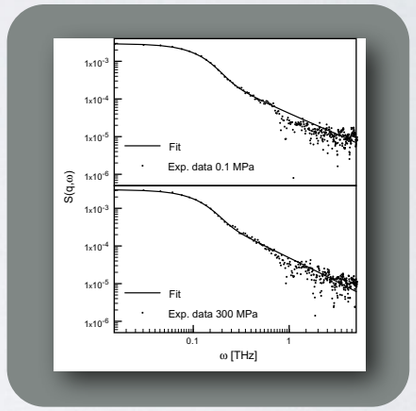

Model development | Detailed analysis | Environment

"Classical" nMoldyn | nMoldyn + McStas

Multiple scattering: example for an undesirable effect

In the MDANSE version of nMoldyn, such effects can be simulated with the McStas instrument simulator

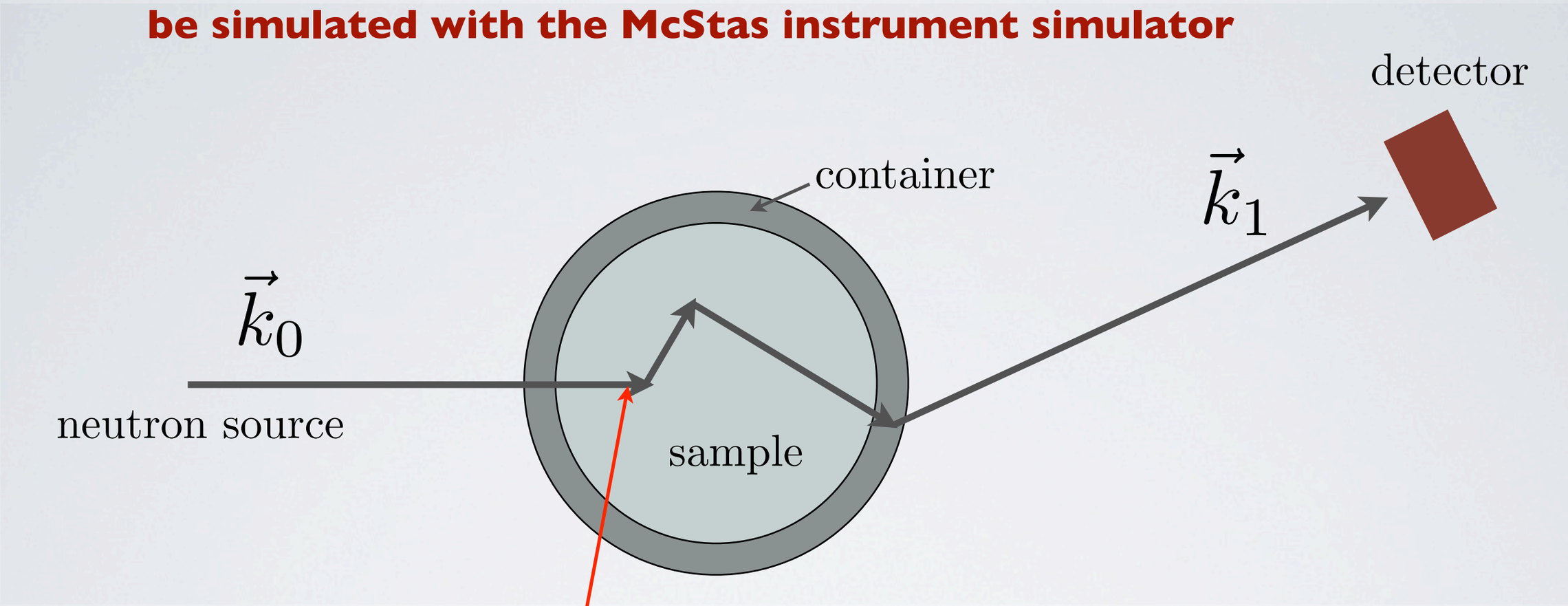

$$\frac{d^2\sigma}{d\Omega d\omega} = \frac{k}{k_0} S(\mathbf{q}, \omega)$$

Differential scatterung cross section for ideal experiment

References

nMoldyn

1. G.R. Kneller, V. Keiner, M. Kneller, and M. Schiller, Comp. Phys. Commun. 91, 191 (1995).
2. T. Rog, K. Murzyn, K. Hinsen, and G.R. Kneller, J Comp. Chem. 24, 657 (2003).
3. V. Calandrini, E. Pellegrini, P. Calligari, K. Hinsen, and G.R. Kneller, Collection SFN 12, 201 (2011).
4. K. Hinsen, E. Pellegrini, S. Stachura, and G.R. Kneller, J Comp. Chem. 33, 2043 (2012).

Other

1. G. R. Kneller, Asymptotic neutron scattering laws for anomalously diffusing quantum particles, J. Chem. Phys, vol. 145, no. 4, pp. 044103–7, 2016.
2. S. Stachura and G. R. Kneller, Probing anomalous diffusion in frequency space. J .Chem. Phys., vol. 143, p. 191103, 2015.
3. G. Kneller, Quasielastic neutron scattering and relaxation processes in proteins: Analytical and simulation-based models, PCCP, vol. 7, pp. 2641 – 2655, 2005.